

**Synthesis of Ternary Nano Composites Based on
ZnCo₂O₄/WS₂/CNTs for High Performance Supercapacitor
Applications**



By

Muhammad Zafar Khan

(Registration No: 00000328833)

Department of Materials Engineering

School of Chemical and Materials Engineering

National University of Sciences & Technology (NUST)

Islamabad, Pakistan

(2024)

**Synthesis of Ternary Nano Composites Based on
ZnCo₂O₄/WS₂/CNTs for High Performance Supercapacitor
Applications**



By

Muhammad Zafar Khan

(Registration No: 00000328833)

A thesis submitted to the National University of Sciences and Technology, Islamabad,

in partial fulfillment of the requirements for the degree of

Master of Science in
Materials and Surface Engineering

Supervisor: Dr. Sofia Javed

School of Chemical and Materials Engineering

National University of Sciences & Technology (NUST)

Islamabad, Pakistan

(2024)

THESIS ACCEPTANCE CERTIFICATE



THESIS ACCEPTANCE CERTIFICATE

Certified that final copy of MS thesis written by Mr **Muhammad Zafar Khan** (Registration No 00000328833), of School of Chemical & Materials Engineering (SCME) has been vetted by undersigned, found complete in all respects as per NUST Statues/Regulations, is free of plagiarism, errors, and mistakes and is accepted as partial fulfillment for award of MS degree. It is further certified that necessary amendments as pointed out by GEC members of the scholar have also been incorporated in the said thesis.

Signature: _____

Name of Supervisor: **Dr Sofia Javed**

Date: 1-10-24

Signature (HOD): _____

Date: 2/10/24

Signature (Dean/Principal): _____

Date: _____

TH - 1

MSE-15-2020

Form TH-1

National University of Sciences & Technology (NUST) MASTER'S THESIS WORK

Formulation of Guidance and Examination Committee (GEC)

Name: Muhammad zafar Khan NUST Reg No: 00000328833
Department: Department of Materials Engineering Specialization: Master of Science in Materials & Surface Engineering
Credit Hour Completed: 24.0 CGPA: 3.88

Course Work Completed

S/No:	Code:	Title:	Core/Elective:	CH:	Grade:
1.	MSE-811	Materials Thermodynamics	Compulsory	3.0	A
2.	MSE-821	Mechanical Behaviour Of Materials	Compulsory	3.0	B+
3.	RM-898	Research Methodology	Additional	2.0	Q
4.	MSE-881	Manufacturing Processes	Compulsory	3.0	A
5.	MSE-812	Phase Transformation & Microstructures	Compulsory	3.0	A
6.	MSE-851	Surface Engineering & Characterisation	Compulsory	3.0	A
7.	ESE-904	Advanced Energy Materials: Synthesis & Characterization	Elective	3.0	A
8.	NSE-842	Nano Materials For Energy Applications	Elective	3.0	A
9.	MSE-941	Materials For High Temperature Applications	Elective	3.0	B+

Date 03 - Nov - 2022

Student's Signature

Thesis Committee

- Name: Sofia Javed (Supervisor)
Department: Department of Materials Engineering
- Name: Iftikhar Hussain Gul (Internal)
Department: Department of Materials Engineering
- Name: Muhammad Irfan (Internal)
Department: Department of Materials Engineering

Signature

Signature

Signature

Date: 03 - Nov - 2022

Signature of Head of Department:

APPROVAL

Date: 03 - Nov - 2022

Signature of Dean/Principal:

School of Chemical & Materials Engineering (SCME) (SCME) H-12 Campus.



National University of Sciences & Technology (NUST)

MASTER'S THESIS WORK

We hereby recommend that the dissertation prepared under our supervision by
Regn No & Name: 00000328833 Muhammad Zafar Khan

Title: Synthesis of Ternary Nano Composites Based on ZnCo₂O₄/WS₂/CNTs for High Performance Supercapacitor Applications.

Presented on: 12 Sep 2024 at: 1500 hrs in SCME Seminar Hall

Be accepted in partial fulfillment of the requirements for the award of Masters of Science degree in **Materials & Surface Engineering.**

Guidance & Examination Committee Members

Name: Dr Muhammad Irfan

Signature: [Signature]

Name: Dr Iftikhar Hussain Gul

Signature: [Signature]

Supervisor's Name: Dr Sofia Javed

Signature: [Signature]

Dated: 23-9-24

[Signature]
Head of Department
Date 26/9/24

[Signature]
Dean/Principal
Date 27/9/24

AUTHOR'S DECLARATION

I Muhammad Zafar Khan hereby state that my MS thesis titled “Synthesis of Ternary Nano Composites Based on ZnCo₂O₄/WS₂/CNTs for High Performance Supercapacitor Applications” is my own work and has not been submitted previously by me for taking any degree from National University of Sciences and Technology, Islamabad or anywhere else in the country/ world.

At any time if my statement is found to be incorrect even after I graduate, the university has the right to withdraw my MS degree.

Name of Student: Muhammad Zafar Khan

Date: 14 June 2024

PLAGIARISM UNDERTAKING

I solemnly declare that research work presented in the thesis titled “Synthesis of Ternary Nano Composites Based on $\text{ZnCo}_2\text{O}_4/\text{WS}_2/\text{CNTs}$ for High Performance Supercapacitor Applications” is solely my research work with no significant contribution from any other person. Small contribution/ help wherever taken has been duly acknowledged and that complete thesis has been written by me.

I understand the zero-tolerance policy of the HEC and National University of Sciences and Technology (NUST), Islamabad towards plagiarism. Therefore, I as an author of the above titled thesis declare that no portion of my thesis has been plagiarized and any material used as reference is properly referred/cited.

I undertake that if I am found guilty of any formal plagiarism in the above titled thesis even after award of MS degree, the University reserves the rights to withdraw/revoke my MS degree and that HEC and NUST, Islamabad has the right to publish my name on the HEC/University website on which names of students are placed who submitted plagiarized thesis.



Student Signature:
Name: Muhammad Zafar Khan

DEDICATION

"All my dedication is to the most loving and caring father(late) and my mother. The thesis is dedicated to my siblings for always believing in me, particularly my brothers who always stood there for me both morally and economically. To my mentors and advisors, whose insight and counsel have been priceless. I want to thank each one of you for helping to make this happen."

ACKNOWLEDGEMENTS

Allah has been kind and merciful, for guiding me throughout my academic journey. Allah has guided me along my academic path with kindness and mercy.

I want to sincerely thank Dr. Sofia Javed, my supervisor, whose knowledge, direction, and steadfast support allowed me to complete my thesis. I sincerely appreciate all your patience and insightful advice during this trip.

I would like to express my sincere gratitude to my GEC members, Dr. Muhammad Irfan, and Dr. Iftikhar Hussain Gul, for their supportive and helpful comments.

I am also appreciative of my friends and coworkers' help, particularly Mr. Marghoob Ahmed.

Finally, I would like to express my sincere gratitude to my family for their unwavering love, support, and inspiration. Without you, this accomplishment would not have been possible.

I want to thank everyone who has contributed to this work.

Muhammad Zafar Khan

TABLE OF CONTENTS

ACKNOWLEDGEMENTS	IX
TABLE OF CONTENTS	X
LIST OF TABLES	XIII
LIST OF FIGURES	XIV
LIST OF SYMBOLS, ABBREVIATIONS AND ACRONYMS	XV
ABSTRACT	XVI
CHAPTER 1: INTRODUCTION	1
1.1 Introduction	1
1.2 Brief Introduction of Energy Storage Devices	1
1.3 Need for Advanced Energy Storage Devices	3
1.4 Introduction to Supercapacitors	4
1.4.1 Fundamentals of Supercapacitors	4
1.4.2 The Origins of Supercapacitors	5
1.4.3 Types of Supercapacitors	6
1.5 Electrode Materials for Supercapacitors	7
1.5.1 Carbon Based Nanostructures	8
1.5.2 Activated Carbons	9
1.5.3 Graphene	10
1.5.4 Functionalized Carbon Nanotubes (CNTs)	10
1.5.5 Transitions Metal Dichalcogenides (TMDs)-2D Materials	11
1.5.6 Sulphides (WS ₂), 2D materials	13
1.5.7 Synthesis of WS ₂	14
1.6 Transition Metal Oxides (TMOs)	16
1.6.1 Simple Transition Metal Oxides (TMOs)	16
1.6.2 Ruthenium dioxide (RuO ₂)	17
1.6.3 Manganese Dioxide	18
1.6.4 Nickel Oxide (NiO)	19
1.6.5 Binary Transition Metal Oxides (BTMOs)	20
1.6.6 Zinc Cobaltate (ZnCo ₂ O ₄)	25
1.7 Composites of WS₂ and ZnCo₂O₄	28
1.7.1 Composites for Improved Performance	28
1.8 Synthesis Routes for Composites of ZnCo₂O₄, WS₂, and Functionalized CNTs	29
1.8.1 Synthesis of ZnCo ₂ O ₄	29
1.8.2 WS ₂ Synthesis	29
1.8.3 Synthesis of Functionalized CNTs	29
1.8.4 Composites of ZnCo ₂ O ₄ /WS ₂ and ZnCo ₂ O ₄ /FCNTs	30

1.9	Challenges of associated WS₂, ZnCo₂O₄ and CNTs as supercapacitor electrode	31
1.9.1.	Challenges of ZnCo ₂ O ₄	31
1.9.2	Challenges of WS ₂	31
1.9.3	Challenges of CNTs	32
1.10	Motivation behind synthesis of ZnCo₂O₄/ WS₂/COOH-CNTs	32
1.11	Hypothesis	33
1.12	Aims and Objectives	33
CHAPTER 2: LITERATURE REVIEW		34
2.1	Carbon and carbon-based supercapacitors	34
2.2	WS₂ and WS₂ based supercapacitors	35
2.3	ZnCo₂O₄ based supercapacitors.	35
CHAPTER 3: MATERIALS AND METHODS		37
3.1	Design of Experiment	37
3.2	Synthesis of ZnCo₂O₄	38
3.2.1	Materials Required	38
3.2.2	Apparatus	39
3.2.3	Synthesis	39
3.3	Synthesis of WS₂	40
3.3.1	Materials Required	40
3.3.2	Apparatus	40
3.3.3	Synthesis	41
3.4	Synthesis of ZnCo₂O₄/WS₂ Composite	42
3.5	Synthesis of ZnCo₂O₄/FCNTs Composite	42
3.6	Synthesis of ZnCo₂O₄/WS₂/FCNTs Composite	42
3.6.1	Materials Required	42
3.6.2	Apparatus	43
3.6.3	Synthesis	43
3.8	Samples Preparation for Electrochemical Testing	44
CHAPTER 4: RESULTS AND DISCUSSION		47
4.1	SEM Analysis	47
4.2	Energy Dispersive X-Ray Spectroscopy	49
4.2.1	EDX results of COOH Functionalized CNTs	49
4.3	BET Results	53
4.4	X-Ray Diffraction Results	54
4.5	FTIR Results	56
4.6	Application testing results	57
4.6.1	Cyclic voltammetry results	58
4.6.2	Galvanometric charge-discharge results	59
4.6.3	Electron Impedance Spectroscopy Results	62
4.6.4	Cyclic Stability and Columbic Efficiency Results	63
CHAPTER 5: CONCLUSIONS AND FUTURE RECOMMENDATION		65
5.1	Conclusion	65

5.2 Future Recommendations

65

REFERENCES

ERROR! BOOKMARK NOT DEFINED.

LIST OF TABLES

Table 1.1: shows the general physical and chemical properties of WS ₂	14
Table 1.2: A comparison of BTMOs and TTMOs	21
Table 1.3: Morphology wise Capacitance of BTMOs salvo-thermally synthesized	24
Table 2.1: Electrochemical properties of different carbon materials[41-43]	34
Table 2.2: Electrochemical properties of various WS ₂ based electrode materials...	35
Table 2.3: Electrochemical properties of ZnCo ₂ O ₄ and its composites	36
Table 4.1: BET surface area, pore width and pore volume values.....	53
Table 4.2: Shows the lattice strain and crystallite size of ZnCo ₂ O ₄	55
Table 4.3: shows the specific capacitance at a scan rate of 5mV/s & 20mV/s.	59
Table 4.4: Specific Capacitance of all the synthesized materials at 0.5A/g.....	60

LIST OF FIGURES

Figure 1.1: Electrochemical Energy Storage Devices	3
Figure 1.2: Basic Schematics of Supercapacitors	5
Figure 1.3: Types of supercapacitors with their differences.....	7
Figure 1.4: Illustration of common materials used as electrode for supercapacitors.	8
Figure 1.5: Schematics of activated carbons, carbon nanotubes and Graphene.	9
Figure 1.6: Schematics of TMCs as electrode materials for supercapacitors	12
Figure 1.7: Synthesis processes of TMDs	12
Figure 1.8: Schematics of the crystal structure of WS ₂	13
Figure 1.9: Electrochemical performance of 2D Transition metal dichalcogenides as supercapacitor electrodes	14
Figure 1.10: Various synthesis mechanisms of WS ₂ nanosheets.....	16
Figure 1.11: Schematics of crystal structure of Co ₃ O ₄ and ZnCo ₂ O ₄	28
Figure 3.1: Schematic illustration of the design of experiment.	38
Figure 3.2: Hydrothermal synthesis of ZnCo ₂ O ₄	40
Figure 3.3: Schematics of synthesis of WS ₂ nanosheets through liquid phase exfoliation	41
Figure 3.4: Schematics of synthesis of ZnCo ₂ O ₄ /WS ₂ /FCNTs composite.....	45
Figure 4.1: SEM results of (a-c) ZnCo ₂ O ₄ , (d) FCNTs, (e & f) bulk WS ₂ and WS ₂ nanosheets, (g & h) ZnCo ₂ O ₄ /WS ₂ , (i) ZnCo ₂ O ₄ /FCNTs & (j-l) ZnCo ₂ O ₄ /WS ₂ /FCNTs	48
Figure 4.2: EDX spectrum and the composition table of COOH-Functionalized CNTs	49
Figure 4.3: EDX spectrum and the composition table of WS ₂ Nanosheets.....	50
Figure 4.4: EDX spectrum and the composition table of ZnCo ₂ O ₄	50
Figure 4.5: Elemental Mapping composition table and EDX spectrum of binary composite ZnCo ₂ O ₄ /FCNTS	51
Figure 4.6: Elemental Mapping composition table and EDX spectrum of binary composite ZnCo ₂ O ₄ /WS ₂	51
Figure 4.7: a) Elemental Mapping of ZnCo ₂ O ₄ /WS ₂ /FCNTs and b) EDX spectrum of ZnCo ₂ O ₄ /WS ₂ /FCNTs.....	52
Figure 4.8: The adsorption isotherm and the pore distribution of the ternary composite ZnCo ₂ O ₄ /WS ₂ /FCNTs.....	54
Figure 4.9: XRD spectrum of all the samples.....	55
Figure 4.10: FTIR results of (a) COOH-FCNTs, (b) ZnCo ₂ O ₄ , (c) WS ₂ and (d) ZnCo ₂ O ₄ /WS ₂ /COOH-FCNTs.....	57
Figure 4.11: CV plots of (a) WS ₂ , (b) FCNTs, (c) ZnCo ₂ O ₄ , (d) ZnCo ₂ O ₄ /WS ₂ , (e) ZnCo ₂ O ₄ /FCNTs and (f) ZnCo ₂ O ₄ /FCNTs/WS ₂	61
Figure 4.12: GCD plots of (a) WS ₂ , (b) FCNTs, (c) ZnCo ₂ O ₄ , (d) ZnCo ₂ O ₄ /WS ₂ , (e) ZnCo ₂ O ₄ /FCNTs and (f) ZnCo ₂ O ₄ /FCNTs/WS ₂	61
Figure 4.13: (a) CV plots of all samples at 20mV/s, (b) GCD plots of all samples at 0.5A/g and (c) EIS Plots	62
Figure 4.14: Cyclic Stability and Coulombic Efficiency.....	63

LIST OF SYMBOLS, ABBREVIATIONS AND ACRONYMS

Ultrasonication	US
Liquid Phase Exfoliation	LPE
Two Dimensional Nanomaterials	2D
N-methyl-2-pyrrolidone	NMP
De-Ionized Water	DIW
Nanomaterials	NM
CV	Cyclic Voltammetry
GCD	Galvanometric Charge Discharge
EIS	Electron Impedance Spectroscopy
SEM	Scanning Electron Microscope
XRD	X-Ray Diffraction

ABSTRACT

Transition metals oxides and their composites with transition metal dichalcogenides (TMDs) and carbonaceous materials have proved good electrochemical properties for supercapacitor application. In this study, we synthesized WS₂ nanosheets via liquid phase exfoliation, ZnCo₂O₄, binary composites of ZnCo₂O₄/WS₂ and ZnCo₂O₄/FCNTs; and a ternary composite of ZnCo₂O₄/WS₂/FCNTs hydrothermally. ZnCo₂O₄/WS₂/FCNTs showed a higher specific capacitance of 1421.93F/g at 5mV/s. The capacitance shown by ZnCo₂O₄/FCNTs, ZnCo₂O₄/WS₂, ZnCo₂O₄, FCNTs and WS₂ at 5mV/s are 1308.45, 1028.59, 788.63, 646.29 and 227.53F/g respectively. The redox current increases with the increasing scan rates. The ternary composite showed the highest integral area and redox peak current values which indicates the availability of more electroactive sites than the binary composites and the individual constituents. The shape of the CV curve suggested a pseudocapacitive nature of the ternary composite. Galvanostatic charge discharge (GCD) was done at current densities of 0.5A/g, 1A/g, 2A/g, and 5A/g. The capacitances shown by ZnCo₂O₄/WS₂/FCNTs, ZnCo₂O₄/FCNTs, ZnCo₂O₄/WS₂, ZnCo₂O₄, FCNTs and WS₂ at a current density of 0.5A/g are 1571, 1210, 1125, 756, 525, and 241 F/g respectively. The electrochemical results suggested the ternary electrode ZnCo₂O₄/WS₂/FCNTs as a better electrode material for supercapacitor applications. The better performance of the ternary composite can be attributed to the synergistic effect of WS₂, FCNTs and ZnCo₂O₄. The integration of functionalized CNTs with ZnCo₂O₄ and WS₂ creates a conductive network that facilitates efficient charge transport, reducing the internal resistance of the electrode. The combination of ZnCo₂O₄'s pseudocapacitance with the double-layer capacitance provided by CNTs and WS₂ results in a higher overall capacitance. WS₂ also contributes additional pseudocapacitance due to its surface redox reactions. CNTs and WS₂ also give mechanical stability preventing the degradation of ZnCo₂O₄. It is also due to the multiple oxidation states of the transition metals W, Co, and Zn.

Keywords: ZnCo₂O₄, WS₂ and COOH-MWCNTs, ZnCo₂O₄/WS₂/FCNTs, Hydrothermal, Liquid phase exfoliation, Electrochemical Properties

CHAPTER 1: INTRODUCTION

1.1 Introduction

The global energy ecosystem is undergoing significant disruption due to the increased demand for clean and renewable energy sources. Using renewable energy sources like solar, wind, and hydropower is now essential to reducing the consequences of climate change and reliance on fossil fuels.[1]. However, there are substantial obstacles to the broad adoption of these renewable energy sources because of their inherent variability and intermittent. It is essential to create cutting-edge energy storage technologies to meet these challenges. Energy storage devices are necessary to ensure the constant delivery of renewable energy, balance energy demand and supply, and preserve grid stability.[2].

Applications ranging from large-scale grid storage systems to small-scale consumer gadgets depend on energy storage devices. These devices facilitate the effective use of renewable energy sources, help to mitigate variations in the energy supply, and offer backup power during blackouts[2]. The energy industry could undergo a revolution thanks to the development of energy storage technologies, which would increase its sustainability, resilience, and efficiency. This chapter provides an overview of energy storage devices, discusses the need for sophisticated storage solutions, and introduces supercapacitors as potentially useful technology[3].

1.2 Brief Introduction of Energy Storage Devices

Energy storage devices are technologies designed to store energy, ensuring a stable and reliable energy supply. These devices come in various forms and serve multiple applications, each with unique characteristics and advantages. [4]. The primary categories of energy storage devices include:

1. Batteries: One of the most popular types of energy storage devices is the battery. Batteries come in various forms, such as lead-acid, nickel-cadmium, nickel-metal hydride, and lithium-ion batteries, and store energy through chemical processes.

Lithium-ion batteries are especially well-liked due to their low self-discharge rates, extended cycle life, and high energy density. Numerous devices, including electric cars, grid storage systems, and portable electronics, rely on lithium-ion batteries for electricity.[5].

2. Supercapacitors: Supercapacitors, sometimes referred to as ultracapacitors or electrochemical capacitors, accumulate energy by electrostatic mechanisms. Their features include fast charging and discharging capabilities, high energy output or power density, and extended lifespan. Supercapacitors, in contrast to batteries, do not depend on chemical processes, rendering them more stable and long-lasting. They are utilized in applications that need rapid surges of energy, such as regenerative braking in electric automobiles and power backup systems.[6].
3. Flywheels: Flywheels accumulate and retain kinetic energy by the rapid rotation of a heavy mass. They are renowned for their exceptional power density and fast supply of energy. Flywheels are used in power quality applications, providing short-term energy storage to stabilize voltage and frequency fluctuations in the power grid.
4. Thermal Energy Storage Devices: Thermal energy storage devices store energy by capturing and storing heat or cold. These systems are used to balance heating and cooling demands in buildings, as well as in industrial processes. Thermal energy storage is employed to store solar energy in concentrated solar power plants for utilization during periods of limited sunshine.
5. Hydrogen Storage: Hydrogen can be stored and used as an energy, which is produced through electrolysis of water. Hydrogen serves as a fuel in fuel cells, enabling the production of electricity, thus offering a sustainable and highly efficient energy solution. Hydrogen storage devices are currently under development for various purposes, including transportation and grid energy storage..[7].
6. The development of these energy storage devices has been driven by the demand for efficient, reliable, and long-lasting storage of energy. Each technology offers unique advantages and is suited for specific applications, contributing to a more flexible and resilient energy system.

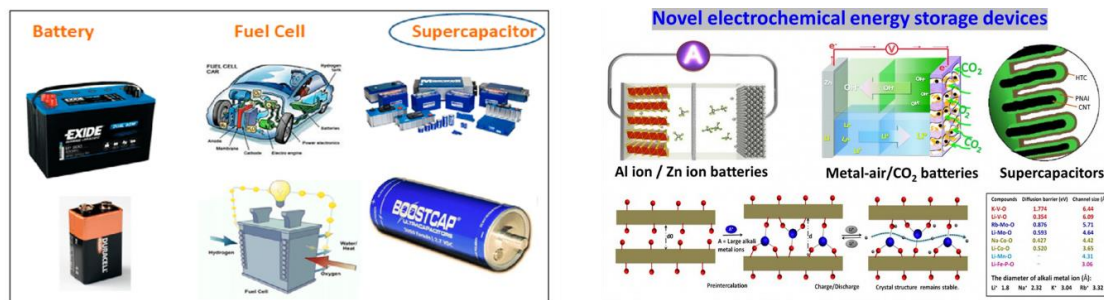


Figure 1.1: Electrochemical Energy Storage Devices[8].

1.3 Need for Advanced Energy Storage Devices

The creation of sophisticated energy storage systems that can overcome the shortcomings of existing technology is important for the shift to a sustainable energy future. The energy storage process which using intermittent renewable sources , including solar and wind, is highlighted by the growing integration of these sources into the electrical grid[9]. Modern energy storage technologies have the following main advantages:

Greater Energy Density: More energy can be stored in a smaller, lighter form factor thanks to advanced energy storage devices' higher energy density. This is especially crucial to reduce the weight in a limited space, such as electric vehicles, and portable appliances.

Longer Cycle Life: Cutting-edge energy storage systems are built to sustain more charge and discharge cycles before experiencing appreciable deterioration. Because of their longer cycle life, energy storage devices are more dependable and economical, requiring fewer replacements over time.

Faster Charge/Discharge Rates: Modern storage systems have faster charge and discharge rates, which facilitate the transfer and recovery of energy more quickly. Applications requiring instantaneous power, like emergency backup, grid stabilization, and regenerative braking in electric vehicles, depend on these capabilities.

Enhanced Stability and Safety: With energy storage systems, safety is the top priority. To reduce the possibility of thermal runaway, leakage, and other risks related to

energy storage devices, cutting-edge technologies are being developed. Improved stability guarantees that storage systems will operate safely in a variety of scenarios.

Environmental Sustainability: Using eco-friendly materials and sustainable manufacturing techniques is a key component of the creation of cutting-edge energy storage systems. A sustainable and cleaner energy system is the aim, and reducing the impact on the environment of energy storage technology helps to achieve this.

The creation of novel materials and energy storage technologies is fueled by the growing need for greener and more effective energy systems. To promote the shift to a low-carbon future, increase the efficiency of energy systems, and allow the broad deployment of renewable energy sources, advanced energy storage technologies are crucial[10].

1.4 Introduction to Supercapacitors

Supercapacitors are such energy storage devices that possess the characteristics of batteries and capacitors. They are also referred to as ultracapacitors or electrochemical capacitors. They store the energy using both the mechanisms i.e., electrostatically, and electrochemically, in contrast to normal capacitors that do so by the electrostatic separation of charges. Supercapacitors outperform conventional capacitors due to their high energy density and longer cycle life because of their dual mechanism[11].

1.4.1 Fundamentals of Supercapacitors

An electrolyte, a separator, and two electrodes make up a supercapacitor. Carbon nanotubes (CNTs), graphene, and activated carbon are examples of materials with a large surface area that are commonly used to make electrodes. Depending on the intended performance characteristics and the application, the electrolyte can be an ionic, organic, or aqueous liquid. Ions can pass through the separator, a porous membrane that keeps the electrodes from coming into touch electrically[12].

Supercapacitors use two main methods to store energy:

- Electric Double Layer Capacitance (EDLC):

Electrostatic charge separation occurs at the electrode-electrolyte contact to store energy. When a voltage is supplied, ions from the electrolyte are attracted to the surface of the electrode, creating an electric double layer. Rapid cycles of charging and discharging are possible thanks to this highly reversible process[13].

- Pseudo capacitance:

Redox reactions that happen quickly and reversibly on electrode surface are the source of pseudo behavior, which store energy. Compared to EDLCs, these reactions produce a greater capacitance because they involve the movement of charge between the electrode and the electrolyte. Because of their high capacitance and redox activity, conducting polymers, transition metal oxides, and metal sulfides are frequently utilized in pseudo capacitors[14].

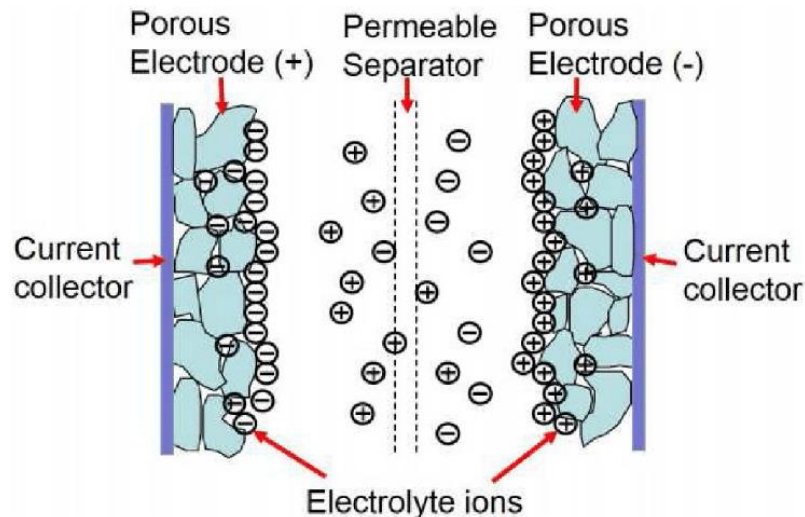


Figure 1.2: Basic Schematics of Supercapacitors[15].

1.4.2 The Origins of Supercapacitors

Supercapacitors were first conceptualized in the 1950s when researchers at General Electric (GE) started investigating the application of porous carbon materials for energy storage. The Standard Oil Company (SOHIO) created the first commercial supercapacitor in the early 1960s using an aqueous electrolyte and activated carbon electrodes. But it

wasn't until the 1990s that supercapacitors became widely used due to important advances in technology and materials.

Supercapacitors now function much better than to the development of new materials including graphene, carbon nanotubes and transition metal oxides. A higher specific surface area, better electrical conductivity, and improved electrochemical stability are the qualities that allow supercapacitors to attain higher power and energy densities. Supercapacitors are being used in various applications, which include grid energy storage and renewable energy systems and electric cars[12].

1.4.3 Types of Supercapacitors

Electric Double Layer Capacitors: EDLCs, or Electric Double-Layer Capacitors, are devices that utilize the process of electrostatic charge separation at the interface between the electrode and electrolyte to store energy. Commonly, electrodes are fabricated using carbon-based materials with large surface areas, such as carbon nanotubes, graphene, or activated carbon. High power density, extended cycle life, and quick charge and discharge times are characteristics of EDLCs. They are frequently utilized in devices that need short bursts of energy, like portable gadgets, regenerative braking in electric cars, and power backup systems[16].

Pseudo capacitors: These devices utilize rapid, reversible redox reactions occurring on the electrode material's surface to store energy. The increased capacitance is a result of the charge transfer occurring between the electrode and the electrolyte in these processes. Ruthenium oxide (RuO₂) and manganese oxide (MnO₂), together with conducting polymers such as polyaniline (PANI) and polypyrrole (PPy), are frequently employed in pseudo capacitors. Pseudo capacitors are utilized in applications that require both high power and high energy density. These capacitors possess a greater energy density compared to EDLCs.[17].

Hybrid Supercapacitors: To obtain better performance, hybrid supercapacitors combine the qualities of EDLCs and pseudo capacitors. They optimize energy storage and distribution by combining several electrode materials. A hybrid supercapacitor, for instance, might have a single electrode material that possesses both double-layer and

pseudo capacitance properties, or it might have an EDLC electrode on one side and a pseudo capacitor electrode on the other. With this arrangement, hybrid supercapacitors can offer longer cycle lives, higher power densities, and higher energy densities than EDLCs. Hybrid supercapacitors are used in industrial power management, renewable energy systems, and electric cars[18]. Figur 3 shows the basic differences between among the three types of supercapacitors

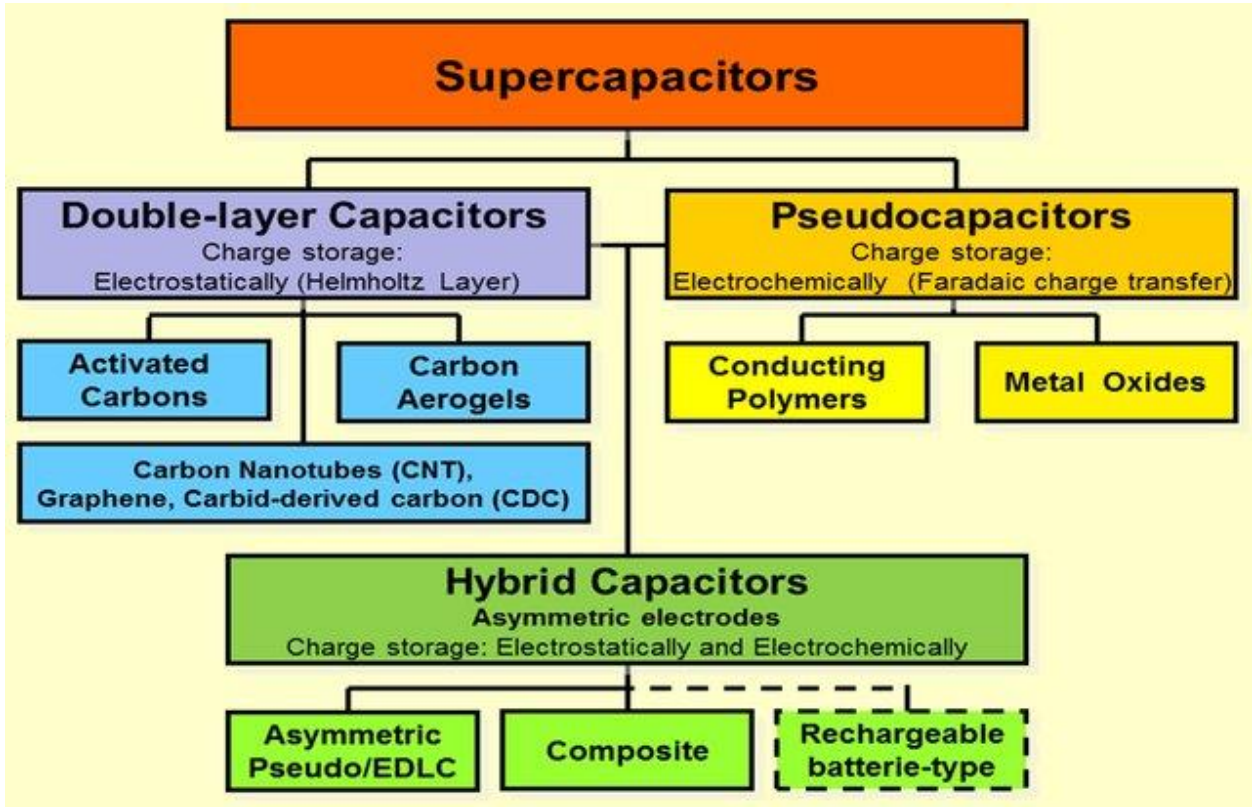


Figure 1.3: Types of supercapacitors with their differences[19].

1.5 Electrode Materials for Supercapacitors

The characteristics of the materials used as electrodes have a major impact on supercapacitors' performance. High surface area, excellent electrochemical stability, superior electrical conductivity, and compatibility with the electrolyte are all desirable qualities in electrode materials. Moreover, the specific capacitance of a supercapacitor is affected or enhanced by controlling some other features like morphology optimization, pore volume, pore shape and pore size distributions, and their availability in an electrolyte.

Designing of a supercapacitor include two main factors (i) selecting a material with high specific surface area to improve the electroactive sites and (ii) manipulating the pore size and shape like spherical, circular, rectangular or square to ease the transportation process. In order to achieve better performance/capacitance, recent research has concentrated on creating and refining a variety of materials, such as Transition metal oxides, sulfides, carbon-based compounds and conductive polymers[20].

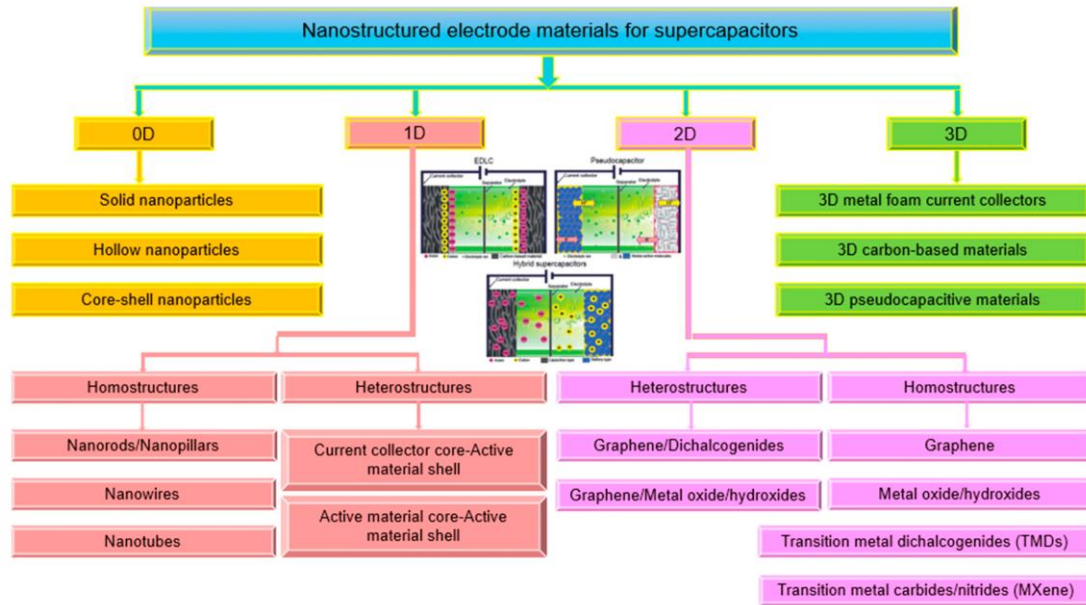


Figure 1.4: Illustration of common materials used as electrode for supercapacitors[21].

1.5.1 Carbon Based Nanostructures

Carbonaceous materials are mostly used as electrode materials for EDLCs due to their selective features like high specific surface area, economics, eco-friendly and their simple synthesis processes. A few of the properties of carbonaceous materials are listed below.

- High surface area
- Smaller pore size
- Thermal stability
- Chemically and electrochemically stable in various electrolytes

- High electrical conductivity

Apart from these properties, surface functionalization is also important which improves specific capacitance of carbon-based electrodes. Carbonaceous electrode materials include carbon aerogels, graphene, activated carbon and carbon nanotubes etc.

Some of the carbonaceous materials are described below.

1.5.2 Activated Carbons

Low cost, better electrical properties and high surface area make AC a suitable material for electrode. It can be synthesized either chemically or physically activating carbon-based materials such as wood, nutshells, wheat straw, rice husk etc. the physiochemical properties of the AC depend on the activation method. In a few cases a high surface area of about $3000\text{m}^2/\text{g}$ can be achieved. Based on the pore size distribution, microporous AC consists of pore ($<2\text{nm}$), mesoporous AC ($2\text{-}50\text{nm}$) and microporous AC consist of pores($>50\text{nm}$).

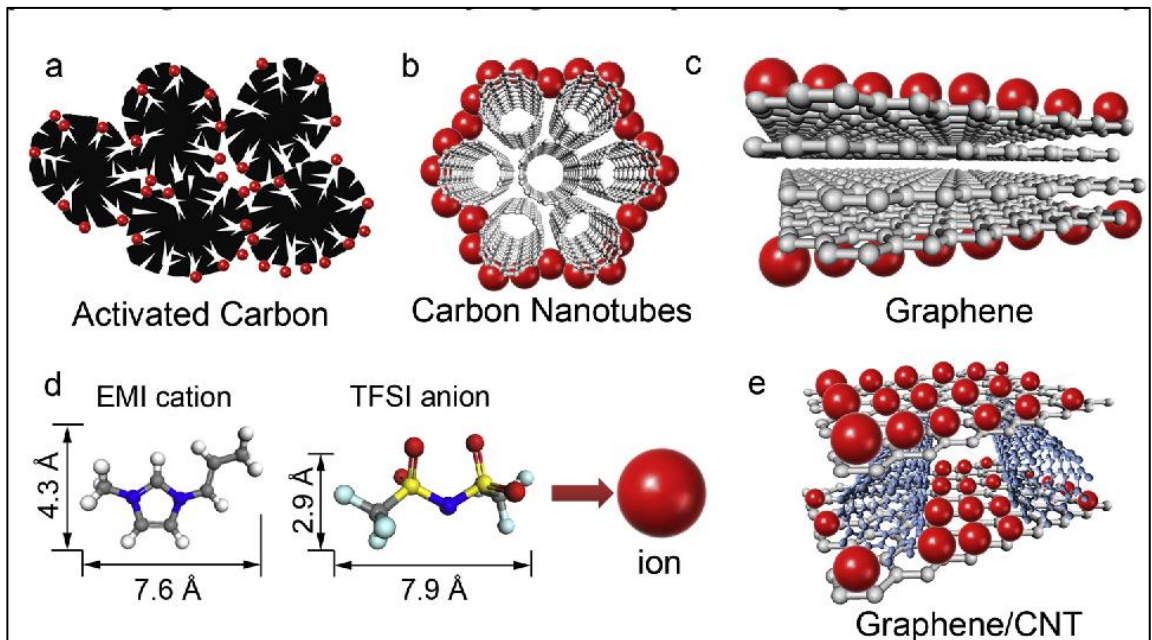


Figure 1.5: Schematics of activated carbons, carbon nanotubes and Graphene[22].

Various studies have shown that having a very high surface area of AC has given less capacitance. This discrepancy is due to the inactivity of all the pores. This means some other parameters are also important while calculating the capacitance of ACs, like the pore distribution. Excessive activation creates large pore volumes which is a drawback as it induces low density and low conductivity, ultimately it will lead to low power and low energy density.

1.5.3 Graphene

Graphene is a 2D or quasi crystal having a promising property for energy storage applications. Various properties include high surface area, chemical stability, and electrical conductivity. Graphene, in solid state doesn't depend on the pore size distribution as compared to ACs or carbon nanotubes. Graphene has a high surface area upto $2650\text{m}^2/\text{g}$. If all available areas are being utilized, graphene can give a capacitance around 550F/g . Also, both the exterior surfaces of graphene are exposed or accessible to the electrolyte, so it can provide all possible active sites to react with the electrolyte.

1.5.4 Functionalized Carbon Nanotubes (CNTs)

Fundamental Characteristics and Uses: Made of rolled-up graphene sheets, carbon nanotubes (CNTs) are cylindrical nanostructures. They have a large specific surface area, are mechanically strong and highly conductive. To increase their characteristics and electrolyte compatibility, functional groups or other materials are added to the surface of carbon nanotubes (CNTs) to create functionalized CNTs. Chemical processes like acid oxidation, which add oxygen-containing groups to the CNT surface (such as carboxyl and hydroxyl), can functionalize the material[23].

Energy Storage Applications: Because of their high electrical conductivity and huge surface area, which enable quick charge and discharge cycles, functionalized CNTs make excellent electrode candidates for supercapacitors. Increased capacitance and improved electrochemical performance are the results of the functional groups on CNTs improving the wettability and contact with the electrolyte. Functionalized carbon nanotubes (CNTs)

can be employed as independent electrode materials or in composites with other materials to improve energy storage[24].

1.5.5 *Transitions Metal Dichalcogenides (TMDs)-2D Materials*

TMDs are compounds constituting groups 3 to 12 elements (transition metals) and group 16 elements like tellurides, selenides, and sulfides. They are stable 2D materials, crystalline compounds and anisotropic in nature. They found themselves in various applications due to their various properties like tunable structures, various band gaps, stoichiometry, and their diversity. Applications include energy conversion and energy storage. Properties which make TMDs promising candidates for supercapacitor are listed below.

- Short diffusion pathways
- Morphological diversity
- More Electrochemically active sites
- Higher flexibility
- Moderate conductivity
- Quantum effect.

Sulphides include, nickel sulphides (NiS, NiS₂, Ni₃S₂, Ni₃S₄, Ni₇S₁₀, and Ni₉S), molybdenum sulphide (MoS₂), cobalt sulphide (CoS, CoS₂, Co₃S₄ and Co₉S₈), ruthenium sulphide (RuS₂) and tungsten sulphide (WS₂), copper sulphide (CuS, Cu₂S, CuS₂, Cu_{1.75}S and Cu_{1.95}S). Selenides include MoSe₂, CuSe, CuSe₂, CoSe, CoSe₂, Co₂Se₃()

Few factors resist the TMCs from achieving higher capacitance values are as below.

- Poor conductivity
- Poor cyclability

- Aggregation issues
- Poor surface area

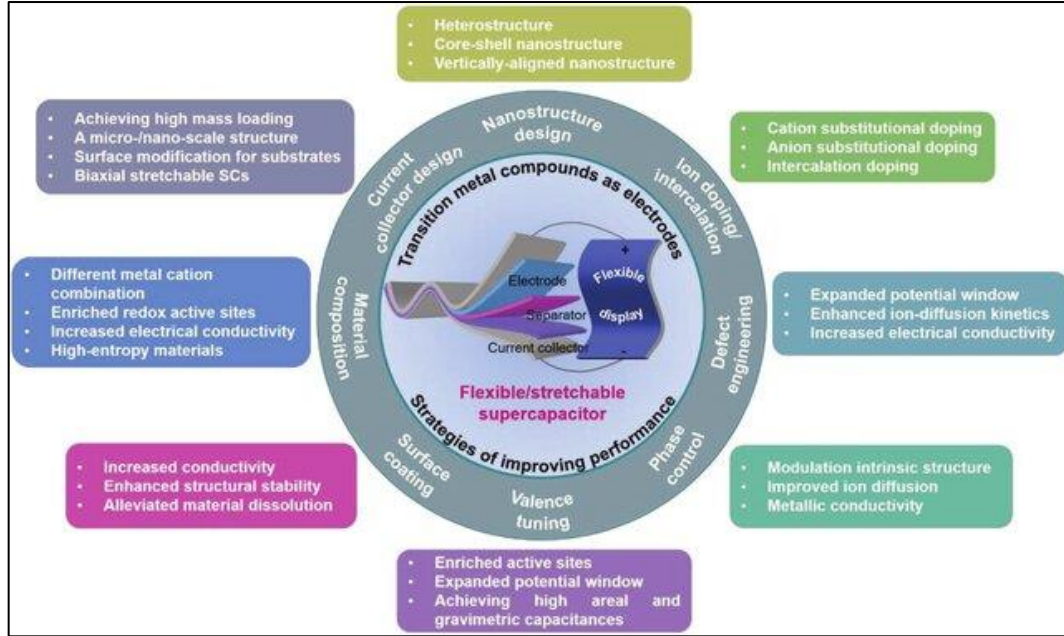


Figure 1.6: Schematics of TMCs as electrode materials for supercapacitors[25].

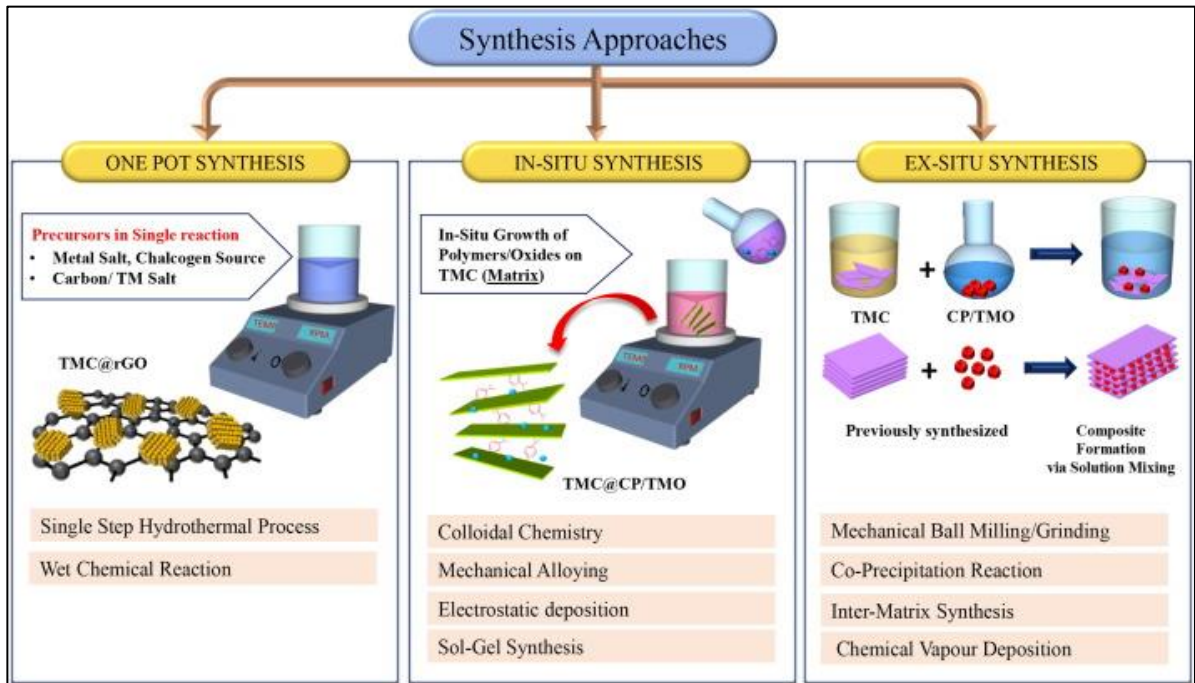


Figure 1.7: Synthesis processes of TMDs[26].

1.5.6 Sulphides (WS_2), 2D materials

Basic Properties and Applications: Graphene-like 2D-layered structure characterizes tungsten disulfide (WS_2), a transition metal dichalcogenide (TMD).

High surface area, strong electrochemical stability, and superior electrical conductivity are all displayed by WS_2 . WS_2 has gained enough attention for energy storage devices due to its layered structure, which allows for the intercalation and removal of ions.[27].

Energy Storage Applications: Because of its high theoretical capacitance and strong cycling stability, WS_2 finds its application in supercapacitor as an electrode. WS_2 's capacity for quick and reversible redox reactions improves its capacity for energy storage. For better performance, WS_2 can be utilized as an electrode material on its own or in composites with other materials.

When carbon-based materials such as graphene or carbon nanotubes (CNTs) are combined with WS_2 , hybrid electrodes with improved capacitance and stability are produced[28]. Various works have been done on the 2D sulphides like MoS_2 , NiS_2 , NiS_2 , Ni_3S_2 , CoS and WS_2 .

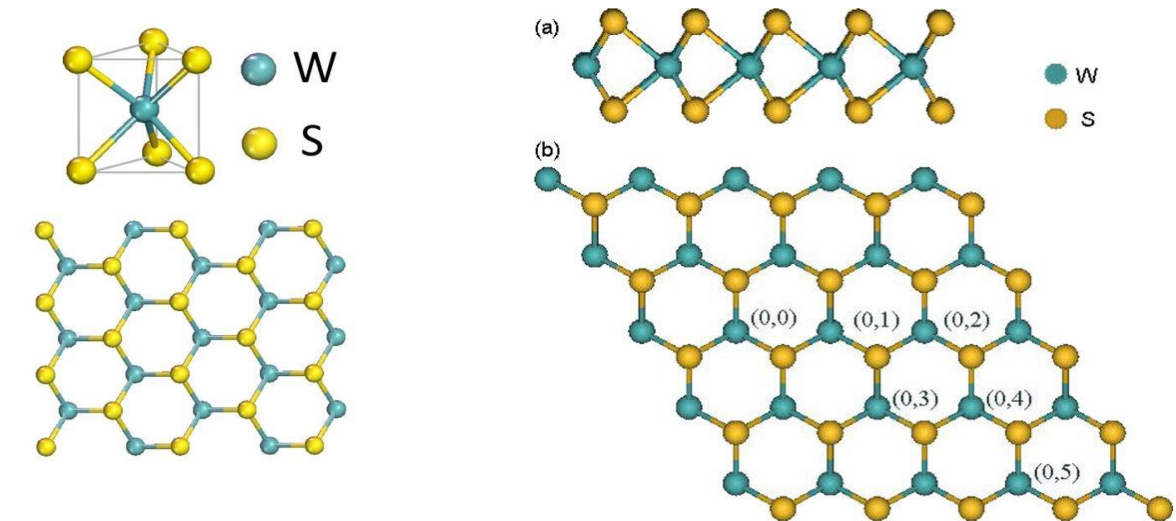


Figure 1.8: Schematics of the crystal structure of WS_2 [29].

TMD Hybrid electrode	Capacitance/Scan rate	Capacitance Retention (%) / Scan rate	Cycles	Energy density	Operation voltage (V)
WS ₂ /rGO	350 Fg ⁻¹ /2 mV/s	100/3 Ag ⁻¹	1000	49 WhKg ⁻¹	-
MoS ₂ /rGO	265 Fg ⁻¹ /10 mV s ⁻¹	92/20 mV s ⁻¹	1000	63 WhKg ⁻¹	0.25-0.8
MoS ₂ /MWCNT	452.7 Fg ⁻¹ /1 Ag ⁻¹	95.8/1 Ag ⁻¹	1000	-	-0.75-0.25
3D Graphene/MoS ₂	169.37 Fg ⁻¹ /1 Ag ⁻¹	90/100 mVs ⁻¹	1400	24.59 Wh/Kg	-0.9-0.2
Porous C/MoS ₂	210 Fg ⁻¹ /1 Ag ⁻¹	105/4 Ag ⁻¹	1000	-	0.0-0.5
Carbon fiber cloth/WS ₂	399 Fg ⁻¹ /1 Ag ⁻¹	99/1 Ag ⁻¹	500	-	-0.8-0.2
MoS ₂ -NiO	1080.6 Fg ⁻¹ /1 Ag ⁻¹	101.9/2 Ag ⁻¹	9000	39.6 Whkg ⁻¹	0.0-0.5
MoS ₂ /NiCo ₂ O ₄	7.1 Fcm ⁻² /2 mVs ⁻¹	98.2/6 Ag ⁻¹	8000	18.4 Whkg ⁻¹	0.0-0.6
WS ₂ /WO ₃	47.5 mFcm ⁻² /5 mVs ⁻¹	≥100/100 mVs ⁻¹	30,000	0.06 Whcm ⁻³	-0.3-0.5
MoS ₂ -CoSe ₂	2577 Fg ⁻¹ /1 Ag ⁻¹	91.03/20 Ag ⁻¹	5000	60.5 Whkg ⁻¹	-0.2-0.8
MoS ₂ /Bi ₂ S ₃	1258 Fg ⁻¹ /30 Ag ⁻¹	92.8/10 Ag ⁻¹	5000	-	-0.2-0.6
MoS ₂ /CoS ₂	142 mFcm ⁻² /1 mAcm ⁻²	92.7/1 mAcm ⁻²	1000	11.11 Whkg ⁻¹	-0.6-0.2
NiSe@MoSe ₂	223 Fg ⁻¹ /1 Ag ⁻¹	91.4/5 Ag ⁻¹	5000	32.6 Whkg ⁻¹	-0.1-0.6
MoS ₂ @3D-Ni-foam	3400 mFcm ⁻² /3 mAcm ⁻²	80/50 mAcm ⁻²	4500	-	0.0-0.6
Ag@MoS ₂	980 Fg ⁻¹ /1 Ag ⁻¹	97/1 Ag ⁻¹	5000	-	-0.1-0.6
3D tubular MoS ₂ /PANI	552 Fg ⁻¹ /0.5 Ag ⁻¹	79/1 Ag ⁻¹	6000	-	-0.1-0.6
1H-MoS ₂ @Oleylamine	50.65 mFcm ⁻² /0.37 Ag ⁻¹	240/2.75 mAcm ⁻²	5000	1-7 μWhcm ⁻²	0.0-1.0
MoS ₂ /PPy	700 Fg ⁻¹ /10 mV s ⁻¹	85/1 Ag ⁻¹	4000	83.3 Whkg ⁻¹	0.0-0.9
MoS ₂ /RGO@PANI	1224 Fg ⁻¹ at 1 Ag ⁻¹	82.5/10 Ag ⁻¹	3000	22.3 Whkg ⁻¹	-0.2-0.8
1D PANI/2D MoS ₂	812 Fg ⁻¹ /1 mAcm ⁻²	-	-	112 Whkg ⁻¹	0.0-1.0

Figure 1.9: Electrochemical performance of 2D Transition metal dichalcogenides as supercapacitor electrodes

General properties of WS₂:

Table 1.1: shows the general physical and chemical properties of WS₂.

Molecular formula	WS ₂
Electronic Configuration of WS ₂	W [Xe] 4f ¹⁴ , 5d ⁴ , 6s ² S [Ne] 3s ² , 3p ⁴
Molar mass	248g/mole
Density	7.5g/cm ³
Melting point	1250 ⁰ C

1.5.7 Synthesis of WS₂

Various synthesis processes have been employed to produce WS₂ nanosheets. Here is an introduction to some of the main synthesis processes:

Mechanical Exfoliation: Mechanical exfoliation is the process of peeling off of thin layers of WS₂ from bulk WS₂ with the help of sticky tapes. This method can produce high-quality nanosheets with minimal defects. However, it is labor-intensive and not scalable for large-scale production.

Liquid Exfoliation: In liquid exfoliation, bulk WS₂ is dispersed in a solvent (such as N-methyl-2-pyrrolidone or water) and subjected to ultrasonic agitation. The van der Waals forces between the layers get broken due to the ultrasonic waves, resulting in exfoliation into nanosheets. Although it is a scalable and simple method, but it often produces nanosheets with a wide range of thicknesses and sizes.

Chemical Vapor Deposition (CVD): CVD involves the reaction of tungsten and sulfur sources at high temperatures to form WS₂ nanosheets on a substrate. This process can produce high-quality and uniform nanosheets with controlled thickness and large lateral size. However, it requires sophisticated equipment and precise control over the reaction conditions.

Hydrothermal/Solvothermal Synthesis: In hydrothermal or solvothermal synthesis, tungsten and sulfur precursors are dissolved in a solvent and reacted under high pressure and temperature in an autoclave. This technique can produce WS₂ nanosheets with good crystallinity and control over morphology. However, the reaction times are relatively long, and the process requires high-pressure equipment.

Chemical Exfoliation: Chemical exfoliation uses intercalation compounds, such as lithium intercalation, to insert ions between the WS₂ layers, which weakens the van der Waals forces and allows for subsequent exfoliation in a solvent. This method can produce large quantities of nanosheets but often results in chemically modified or defect-rich materials.

Sol-Gel Method: The sol-gel method involves the transition of a solution (sol) into a solid (gel) to form WS₂ nanosheets. Typically, tungsten precursors are dissolved and then reacted with sulfur sources in solution, followed by gelation and drying. This method can be used for large-scale production, but it may require post-synthesis treatments to improve the quality of the nanosheets.

Electrochemical Exfoliation: In electrochemical exfoliation, a WS₂ electrode is subjected to an electric field in an electrolyte solution, causing the layers to separate into nanosheets. This technique is relatively fast and can produce high-quality nanosheets, but it requires a controlled electrochemical setup. Each synthesis method has its own trade-offs in terms of scalability, quality of nanosheets, cost, and complexity. Selection of method depends on the requirements of the need and available resources.

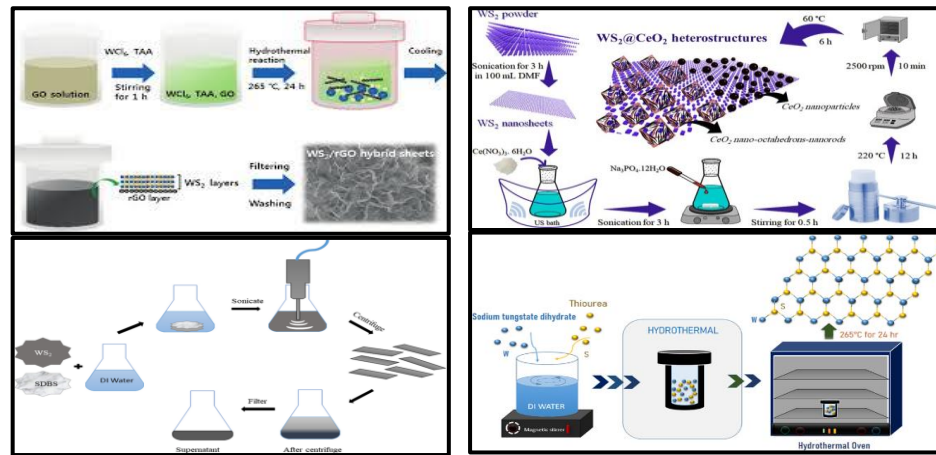


Figure 1.10: Various synthesis mechanisms of WS₂ nanosheets[30].

1.6 Transition Metal Oxides (TMOs)

TMOs are of two types i.e., simple transition metal oxides and Binary transition metal oxides. They both are important electrode materials for supercapacitor applications. Various works have been done on their usage in energy storage devices.

Both have their own merits and demerits.

1.6.1 Simple Transition Metal Oxides (TMOs)

Composition:

Simpler Structure: Consist of one transition metal and oxygen. Examples: MnO₂ (Manganese oxide), NiO (Nickel oxide), RuO₂ (Ruthenium oxide).

Advantages:

1. **Chemical and Thermal Stability:** The simpler structure often leads to high stability.
2. **Well-Understood Properties:** Due to their simpler composition, their electrochemical properties are well-studied and predictable.
3. **Ease of Synthesis:** Generally easier and less expensive to synthesize compared to BTMOs.

Disadvantages:

1. **Limited Performance:** May have lower specific capacitance and conductivity compared to TTOs.
2. **Single Functionality:** Limited to the properties of one type of metal ion, which can restrict performance enhancement.

Metal oxides proved to be the promising candidates for electrode materials for supercapacitors applications. They have a unique property of low resistance which offer a high specific capacitance.

Moreover, it offers high energy density and power density. Ruthenium dioxide (RuO_2), manganese oxide (MnO_2), iridium oxide (IrO_2), nickel oxide (NiO) are the commonly used metal oxides. Some binary oxides are described below.

1.6.2 Ruthenium dioxide (RuO_2)

Due to its excellent electrochemical properties, ruthenium oxide (RuO_2) is a highly demanded electrode material for supercapacitors. Properties of RuO_2 that make it include:

1. **High Specific Capacitance:** RuO_2 offers the highest specific capacitances due to its ability to store charge through both faradaic (pseudocapacitive) and non-faradaic (electric double-layer) mechanisms.

2. Conductivity: Its electrical conductivity is comparatively high, due to which fast charge transport takes place and reduces energy loss during charge/discharge cycles.
3. Stability: RuO₂ is chemically stable in a various electrolyte, ensures the long-term reliability and capacitance retention.
4. Wide Potential Window: The wide operating window ensures the high energy density of supercapacitors.

Beside this, the commercial use of ruthenium is less because of its high cost and scarcity.

Therefore, work is being done to improve the performance of RuO₂-based electrodes and to replace them with some other alternatives which are cost-effective with similar attributes.

1.6.3 Manganese Dioxide

Manganese oxide (MnO₂), is cheap and has favorable electrochemical properties, thus used as an electrode material in supercapacitors.

1. High Specific Capacitance:

It shows pseudocapacitive behavior. high charge storage is due to its multiple oxidation states during the redox reactions in the cyclic charge-discharge.

2. Abundance and Low Cost:

In comparison with ruthenium oxide, manganese is abundant and cheap, thus MnO₂ is a cost-effective material for supercapacitor applications.

3. Environmental Friendliness:

MnO₂ is environmentally non-toxic material, thus its usage is beneficial.

4. Good Electrochemical Stability:

MnO₂ provides reasonable stability over numerous charge/discharge cycles, maintaining its performance and making it suitable for long-term applications.

5. Wide Potential Window:

Wide operating window attributes a high charge storage capacity of MnO₂. Relatively low electrical conductivity of MnO₂ hinders its performance. To avoid this, composites and hybrid materials are made that combine MnO₂ and conductive materials (like carbon nanotubes or graphene) so its conductivity may be enhanced.

1.6.4 *Nickel Oxide (NiO)*

Because of its electrochemical characteristics, nickel oxide (NiO) is a well-known electrode material for supercapacitors. Among the essential qualities of NiO few are mentioned below:

Elevated Specific Capacitance:

NiO has robust pseudocapacitive characteristics, facilitating effective charge retention via reversible faradaic redox processes. High specific capacitance values result from this, which increases the amount of energy that can be stored.

Excellent Electrical Conductivity:

NiO has adequate electrical conductivity, which makes it easier for charges to move between electrodes and improves the overall performance of supercapacitors.

Cost Effectiveness:

NiO is an economically feasible choice for large-scale applications since nickel is more plentiful and cost-effective when compared to other transition metals.

Chemical Stability:

NiO has strong thermal and chemical stability, which guarantees its reliability.

Environmental Compatibility:

NiO is usually non-toxic and friendly to the environment, which fits nicely with the expanding need for ecologically acceptable energy storage options.

NiO has several drawbacks despite these benefits, including reduced conductivity in comparison to materials based on carbon and possible problems with cycle stability. Research frequently focuses on forming NiO composites with conductive elements, such as graphene or carbon nanotubes, to get around these restrictions and improve the material's endurance and electrochemical performance.

1.6.5 Binary Transition Metal Oxides (BTMOs)

Composition:

- **Complex Structure:** They contain two different transition metals combined with oxygen.
- **Examples:** NiCo₂O₄ (Nickel cobaltite), ZnMn₂O₄ (Zinc manganese oxide), CoMn₂O₄ (Cobalt manganese oxide) and ZnCo₂O₄.

The synergistic effect of different metal ions enhances the electrochemical performance leading to:

- higher values of specific capacitance
- better electrical conductivity
- long cyclic stability

Moreover, adjusting the composition of BTMOs and optimizing their processing can lead to better performance as an electrode material for supercapacitors. Introducing many cations can induce multifunctionality to BTMOs which can make them favorable for various applications.

They are more complex in structure, thus are very difficult to synthesize which makes them costly also. These complex structures sometimes make it difficult to reproduce them.

Detailed comparison of TMOs and BTMOs:

Table 1.2: A comparison of BTMOs and TTMOs

Property	TMOs	BTMOs
Performance	<ul style="list-style-type: none"> • less versatility in tuning properties • poor/lower electrical conductivity • highly stable and high specific capacitance 	<ul style="list-style-type: none"> • higher specific capacitance and conductivity • synergistic effects make them more conductive
Cost/scalability	More cost-effective and easier to scale up	Expensive and complex to produce
Application potential	Applicable where cost and simplicity are critical, and the performance requirements are moderate.	High-performance applications where enhanced electrochemical properties justify the higher cost and complexity
Material availability	derived from more abundant and less expensive metals	metals that might be less abundant or more expensive

Various BTMOs are listed below with their pros and cons.

Nickel Cobalt Oxide (NiCo₂O₄)

- Advantages:

High specific capacitance (~2500 F/g), excellent electrical conductivity, and synergistic effects from both nickel and cobalt that enhance the electrochemical performance.

- Challenges:

Relatively complex synthesis methods and potential stability issues under prolonged cycling.

Nickel Manganese Oxide (NiMn₂O₄)

- Advantages:

High specific capacitance, good electrochemical stability, and a combination of redox activities from both nickel and manganese.

- Challenges:

Poor intrinsic electrical conductivity, requiring combination with conductive additives to achieve optimal performance.

Cobalt Manganese Oxide (CoMn₂O₄)

- Advantages:

High specific capacitance, good electrical conductivity, and the ability to exploit the redox behavior of both cobalt and manganese.

- Challenges:

Synthesis complexity and potential phase instability under repeated cycling.

Zinc Cobalt Oxide (ZnCo₂O₄)

- Advantages:

High specific capacitance, good electrical conductivity, and a relatively straightforward synthesis process.

- Challenges:

Stability issues during long-term cycling and the need for structural optimization to enhance performance.

Copper Cobalt Oxide (CuCo₂O₄)

- Advantages:

High specific capacitance, excellent electrical conductivity, and effective utilization of both copper and cobalt's redox properties.

- Challenges:

Potential aggregation of nanoparticles, which can reduce active surface area and cycling stability.

Copper Manganese Oxide (CuMn₂O₄)

- Advantages: High specific capacitance, good electrochemical stability, and a synergistic enhancement of electrochemical properties from copper and manganese.
- Challenges: Lower electrical conductivity compared to other ternary oxides, requiring the incorporation of conductive materials.
- The electrochemical properties of the BTMOs depend on various factors like morphology, particle size, shape, pore size, pore shape etc. The said properties again depend on the synthesis routes of the BTMOs.

Table 1.3: Morphology wise Capacitance of BTMOs salvo-thermally synthesized

Electrode/Morphology of	Conditions	Specific Capacitance
NiCo ₂ O ₄ (urchin structures)	Hydrothermal at 100 ⁰ C for 48 hrs.	658 F/g at 1A/g
Nanowires of NiCo ₂ O ₄	Hydrothermal at 120 ⁰ C for 6 hrs.	2681 F/g at 2A/g
NiCo ₂ O ₄ (urchin structures)	Hydrothermal at 100 ⁰ C for 6 hrs.	1650 F/g at 2A/g
NiCo ₂ O ₄ (hierarchical porous)	NMP-H ₂ O at 180 ⁰ C for 6hrs	1550 F/g at 4A/g
Nanoplates of CoMoO ₄ on Ni foam	Hydrothermal at 180 ⁰ C for 12hrs	1.26 F/cm ² at 4mA/cm ²)
CoMoO ₄ on graphene foam	Hydrothermal at 150 ⁰ C for 5hrs	2731 F/g at 1.43A/g
3D microspheres of NiCo ₂ O	H ₂ O-ethanol at 100C for 6 hrs.	1284 F/g at 2A/g

Various synthesis processes of BTMOs include.

1. Hydrothermal/solvothermal synthesis.
2. Microwave assisted method.
3. Electrodeposition method.
4. Template method
5. Sol-gel method
6. Coprecipitation method

Among all hydrothermal, sol-gel and coprecipitation methods are the commonly used techniques for the synthesis of BTMOs.

1.6.6 Zinc Cobaltate ($ZnCo_2O_4$)

Fundamental Characteristics and Uses: Due to their strong electrochemical performance, high theoretical capacitance, and good electrical conductivity, transition metal oxides (TMOs) are being researched extensively. With its distinct spinel structure and numerous oxidation states, zinc cobaltate ($ZnCo_2O_4$) is a mixed metal oxide that enables high capacitance and energy density. $ZnCo_2O_4$ has a large surface area, strong thermal stability, and excellent electrical conductivity[31].

Energy Storage Applications: Because of its high specific capacitance and steady electrochemical performance, $ZnCo_2O_4$ is used as an electrode in supercapacitors. $ZnCo_2O_4$'s spinel structure makes it ideal for high-performance supercapacitors since it facilitates effective charge storage and transfer. $ZnCo_2O_4$ can be utilized as an electrode material on its own or in composites with other materials to improve energy storage. $ZnCo_2O_4$ with carbon-based materials, including graphene or carbon nanotubes, when combined, produce hybrid electrodes that have higher stability and capacitance[32].

$ZnCo_2O_4$ is environmentally friendly and is abundant in nature thus making it cost effective. It behaves like a p-type semiconductor which affects its electrical conductivity. It possesses a spinel crystal structure like Co_3O_4 . Co^{2+} are replaced by Zn^{2+} ions where Co^{2+} occupies the tetrahedral sites and Zn^{2+} occupies the octahedral sites which leads to much enhanced redox reactions. The intrinsic poor conductivity and large volume change during the charge discharge processes are the disadvantages of $ZnCo_2O_4$. This intrinsic electrical insulation results in rapidly diminishing capacitance at higher current densities and during charge/discharge cycles, typically leading to low-rate capability and poor cycling stability. To overcome these limitations, it is crucial to design suitable electrode materials rationally, as their electrochemical performance is highly dependent on their mechanical properties. To enhance the performance of electrodes based on $ZnCo_2O_4$ for supercapacitor applications, it is essential to achieve an optimized morphology that offers

a high active surface area, short ion and electron diffusion paths, and high diffusion rates. Additionally, the electrode should provide plenty of redox sites.

Crystal Structure of ZnCo₂O₄:

ZnCo₂O₄ is a transition metal oxide with a spinel crystal structure. The spinel structure is a common crystalline form for many transition metal oxides and has the general formula AB₂O₄, where "A" and "B" represent different metal cations. Here, Zn represents the "A" site cation and Co represents the "B" site cation.

Key Features of the ZnCo₂O₄ Spinel Structure:

1. Crystal System: ZnCo₂O₄ crystallizes in the cubic crystal system.
2. Space Group: The space group for ZnCo₂O₄ is $Fd\bar{3}m$ (No. 227).

Atomic Arrangement:

- Tetrahedral Sites (A sites): In the spinel structure, Zn²⁺ ions occupy one-eighth of the available tetrahedral sites. Each tetrahedral site is coordinated by four oxygen atoms.
- Octahedral Sites (B sites): Co³⁺ ions occupy half of the octahedral sites. Each octahedral site is coordinated by six oxygen atoms.
- Oxygen Atoms: The oxygen atoms form a cubic close-packed lattice, and the metal cations are located within the interstices of this lattice.

Coordination:

- Tetrahedral Coordination: Zn²⁺ ions are surrounded by four O²⁻ ions, forming ZnO₄ tetrahedra.
- Octahedral Coordination: Co³⁺ ions are surrounded by six O²⁻ ions, forming CoO₆ octahedra.

Structure Summary:

- The spinel structure can be visualized as a combination of ZnO_4 tetrahedra and CoO_6 octahedra sharing oxygen atoms.
- The general arrangement provides a robust and stable crystal framework, which is beneficial for the material's structural integrity during electrochemical processes.

Importance in Supercapacitors:

- **High Surface Area:** The spinel structure allows for a high density of active sites for redox reactions.
- **Ion and Electron Diffusion:** The arrangement of the tetrahedral and octahedral sites facilitates efficient pathways for ion and electron diffusion, which is crucial for high-rate supercapacitor applications.
- **Mechanical Stability:** The three-dimensional network of the spinel structure contributes to good mechanical stability, which is essential for long-term cycling stability in supercapacitors.

Understanding the crystal structure of ZnCo_2O_4 is vital for designing and optimizing electrode materials, as the electrochemical properties are inherently linked to the atomic arrangement and coordination within the crystal lattice.

To overcome the individual weaknesses and disadvantages of WS_2 and ZnCo_2O_4 , research has been done on their composites with each other and with other materials. Recently, composites of WS_2 and ZnCo_2O_4 have been developed by many researchers and improved electrochemical properties have been achieved. Also, composites of ZnCo_2O_4 and carbon-based materials have been synthesized.

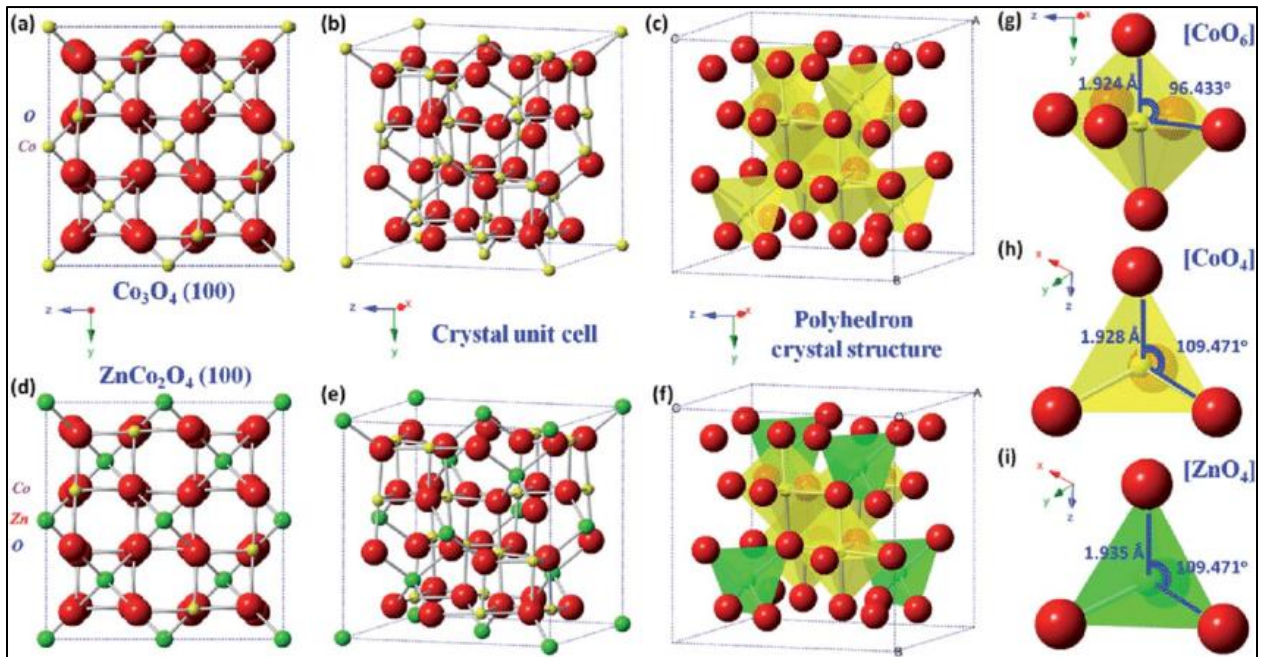


Figure 1.11: Schematics of crystal structure of Co_3O_4 and ZnCo_2O_4 [34].

1.7 Composites of WS₂ and ZnCo₂O₄

1.7.1 Composites for Improved Performance

To obtain better electrochemical performance, composites including functionalized carbon nanotubes, WS₂, and ZnCo₂O₄ combine the benefits of each constituent. By combining the advantages of several materials, such as high stability and low capacitance, these composites seek to overcome the drawbacks of each one. For instance, CNTs can be combined with metal sulphides like WS₂ or oxides like ZnCo₂O₄ to create electrodes that have greater of surface area, high conductivity, and enhanced redox activity[35].

Although these composites function well, there are still several unanswered questions. These include increasing the manufacturing of these materials for use in commercial applications, improving our understanding of the interactions between the various components in the composite, and optimizing synthesis techniques to produce homogeneous and evenly distributed composites. The main goals of current research are to use novel material design and synthesis processes to increase the energy density, power density, and cycle life of supercapacitors. Additionally, the widespread use of these

cutting-edge materials depends on the development of economical and ecologically friendly synthesis techniques[36].

1.8 Synthesis Routes for Composites of ZnCo₂O₄, WS₂, and Functionalized CNTs

1.8.1 Synthesis of ZnCo₂O₄

Several procedures, such as co-precipitation, sol-gel, and hydrothermal approaches, can be used to synthesize ZnCo₂O₄. Precursors for zinc and cobalt react in an aqueous solution at high pressure and high temperature during hydrothermal synthesis, producing well-defined nanostructures. In the sol-gel method, a solution containing metal precursors is formed into a gel, which is then dried and calcined to produce ZnCo₂O₄ nanoparticles. Co-precipitation is the process of precipitating cobalt and zinc hydroxides simultaneously, followed by thermal processing to produce ZnCo₂O₄[37].

1.8.2 WS₂ Synthesis

Chemical vapour deposition (CVD), hydrothermal synthesis, and mechanical exfoliation are three methods that can be used to synthesise WS₂. To create WS₂ films or nanostructures, CVD entails reacting tungsten and sulphur precursors in a high-temperature reactor. WS₂ nanostructures are produced by hydrothermal synthesis, which is the reaction of tungsten precursors with sulphur sources in an aqueous solution at high pressure and temperature. By applying mechanical forces, WS₂ layers are physically separated from bulk crystals during mechanical exfoliation[38].

1.8.3 Synthesis of Functionalized CNTs

CNTs can be made functional by applying functional groups to their surface by chemical processes including acid oxidation. Acid oxidation is the process of treating carbon nanotubes (CNTs) with strong acids, like sulfuric or nitric acid, to introduce functional groups that include oxygen, like carboxyl and hydroxyl groups. These functional groups improve the electrochemical performance of CNTs by increasing their wettability and contact with the electrolyte[39].

ZnCo₂O₄, WS₂, and functionalized carbon nanotubes are combined in a variety of ways during the synthesis of composites, including layer-by-layer assembly, physical mixing, and in situ growth. In situ growth produces well-dispersed and interconnected composites by allowing multiple materials to develop simultaneously during a single synthesis process. Physical mixing is the process of mechanically combining several materials, which is then treated chemically or thermally to create composites. In order to create layered structures with regulated composition and thickness, layer-by-layer assembly entails the sequential deposition of several materials[40].

1.8.4 Composites of ZnCo₂O₄/WS₂ and ZnCo₂O₄/FCNTs

ZnCo₂O₄ is combined with either WS₂ or functionalized CNTs to create hybrid structures that have improved properties. This process is known as ZnCo₂O₄/WS₂ and ZnCo₂O₄/functionalized CNTs (FCNTs) composite synthesis. These composites are made by techniques like electrochemical deposition, solvothermal procedures, and hydrothermal synthesis [41]. ZnCo₂O₄ nanostructures, for instance, can be grown via hydrothermal synthesis on the surface of functionalized CNTs or WS₂ nanosheets to create composite materials with a large surface area, strong electrical conductivity, and improved electrochemical performance. Similarly, well-dispersed and linked composites can be created via solvothermal methods and electrochemical deposition, which can then be optimized for better supercapacitor performance in terms of both structural and electrochemical properties[42, 43]. Mostly coprecipitation and hydrothermal methods have been employed to synthesize the ZnCo₂O₄ following by adding the CNTs or WS₂ in it[44, 45]

Ternary Composites: Ternary composites combine three distinct materials to produce synergistic effects and improve supercapacitor performance even further. A lot of work has been done on the binary composites of TMOs and carbonaceous compounds, and also with WS₂. composites of NiCo₂O₄ and WS₂ have been developed.[44, 46] For instance, the high conductivity of CNTs, the layered structure of WS₂, and the high capacitance of ZnCo₂O₄ can all be combined to create ternary composites of ZnCo₂O₄, WS₂, and functionalized CNTs that have higher energy storage capacities. In order to

attain the intended performance characteristics, the synthesis of ternary composites entails optimizing the composition, structure, and morphology of the various constituents[47].

1.9 Challenges of associated WS₂, ZnCo₂O₄ and CNTs as supercapacitor electrode

Various challenges are associated with WS₂, ZnCo₂O₄ and CNTs as electrode materials for supercapacitor applications. Details are given below.

1.9.1. Challenges of ZnCo₂O₄

- Low electrical conductivity: ZnCo₂O₄ has relatively low intrinsic electrical conductivity, which can hinder electron transport within the electrode material, leading to poor rate performance and lower power density[48].
- Volume expansion and contraction: During the charge-discharge cycles, ZnCo₂O₄ undergoes significant volume changes, which can cause structural degradation, loss of electrical contact, and reduced cycling stability.
- Agglomeration of Particles: ZnCo₂O₄ nanoparticles tend to agglomerate due to high surface energy, leading to a reduction in the available surface area and active sites for electrochemical reactions. This can significantly decrease the material's overall capacitance.
- Synthesis complexity: The synthesis of high-quality ZnCo₂O₄ with controlled morphology and size distribution can be complex and costly, which poses a challenge for large-scale production and commercialization.

1.9.2 Challenges of WS₂

- Intrinsic Low Conductivity: While WS₂ has better conductivity than many transition metal oxides, its intrinsic electrical conductivity is still relatively low compared to other materials like graphene or carbon nanotubes, limiting its rate performance.
- Mechanical Stability: WS₂ can suffer from mechanical instability, such as cracking and pulverization, during charge-discharge cycles. This can lead to a decrease in performance and shortened lifespan of the supercapacitor.

- Restacking and Aggregation: WS₂ nanosheets tend to restack and aggregate due to van der Waals interactions, which reduces the accessible surface area and hinders ion diffusion, thereby lowering the capacitance.

1.9.3 Challenges of CNTs

- Aggregation and Dispersion: NTs tend to agglomerate, and form bundles due to strong van der Waals forces between individual tubes. This aggregation can reduce the effective surface area available for electrochemical reactions and hinder ion accessibility.
- Surface Functionalization: The inert nature of pristine CNTs can limit their electrochemical activity. Surface functionalization can introduce defects and functional groups that enhance pseudocapacitance but may also degrade the electrical conductivity and mechanical properties of the CNTs.
- Cost and Scalability: The synthesis of high-quality CNTs can be expensive and producing them at a large scale with consistent properties remains a significant challenge. This impacts the commercial viability of CNT-based supercapacitors.

1.10 Motivation behind synthesis of ZnCo₂O₄/ WS₂/COOH-CNTs

Developing a composite of ZnCo₂O₄, WS₂, and carboxyl-functionalized CNTs (COOH-CNTs) leverages the unique strengths of each component to enhance supercapacitor performance. ZnCo₂O₄ contributes high pseudo capacitance through its faradaic redox reactions, though it suffers from low electrical conductivity and structural changes during cycling. WS₂, with its good electrical conductivity and additional pseudo capacitance, tends to restack, reducing surface area. COOH-CNTs mitigate these issues by providing exceptional electrical conductivity and mechanical strength, forming a robust conductive network that maintains structural integrity and prevents particle agglomeration. The functional groups on COOH-CNTs improve dispersion and interaction with the electrolyte, enhancing ion accessibility and ensuring rapid charge-discharge cycles. This synergistic combination results in a composite material with higher

energy and power densities, offering scalable, cost-effective solutions for advanced supercapacitor applications in portable electronics and large-scale energy storage systems.

1.11 Hypothesis

The integration of ZnCo_2O_4 , WS_2 , and carboxyl-functionalized CNTs (COOH-CNTs) into a ternary composite will synergistically enhance the electrochemical performance of supercapacitors by combining the high pseudo capacitance of ZnCo_2O_4 and WS_2 with the superior electrical conductivity and structural stability provided by COOH-CNTs, resulting in a composite with improved specific capacitance, enhanced charge-discharge rates, and superior cycling stability.

1.12 Aims and Objectives

- To synthesize a $\text{ZnCo}_2\text{O}_4/\text{WS}_2$, binary composites ($\text{ZnCo}_2\text{O}_4/\text{WS}_2$, $\text{ZnCo}_2\text{O}_4/\text{COOH-CNTs}$) and ternary composite $\text{ZnCo}_2\text{O}_4/\text{WS}_2/\text{COOH-CNTs}$ with uniform dispersion using hydrothermal synthesis
- To characterize the synthesized materials using XRD, EDX, SEM, FTIR.
- To evaluate the electrochemical performance of all the materials synthesized.

Electrochemical testing includes:

- Cyclic voltammetry
 - Galvanometric charge-discharge
 - Electron impedance spectroscopy
 - Cyclic stability
- To compare the electrochemical performance of each with each other.

CHAPTER 2: LITERATURE REVIEW

Various research has been done to overcome the low energy density of supercapacitors, although they possess a very fast charge-discharge cycle with high power density.

2.1 Carbon and carbon-based supercapacitors

Carbonaceous materials include Activated carbons, graphene, carbon nanotubes etc. they possess high surface area, higher conductivity, smaller pore size and better thermal and electrochemical stability, due to which they are being used as electrode materials for supercapacitors.[8, 23, 39, 49]. Different carbon-based materials offer different electrochemical properties.

Table 2.1: Electrochemical properties of different carbon materials[50-52]

Electrode	Capacitance	Electrolyte	Electrode
WS ₂ /carbon fiber	399F/g at 1A/g	1 M KOH	99% after 500 cycles [50]
WS ₂ /encapsulated amorphous carbon tubes	539F/g at 1A/g	3M KOH	60% after 500 cycles[50]
MoS ₂ -carbon composite	201.4F/g at 0.2A/g	3M KOH	94.1% after 1000 cycles at 1.6A/g
Polypyrrole/graphene	373.2 mF/cm ² , 0.5 mA/cm ²	PVA/KCl hydrogel	96.8% after 10k cycles

2.2 WS₂ and WS₂ based supercapacitors.

Different morphologies of WS₂ have shown different electrochemical properties. Hierarchical structure of graphene and 2D WS₂ has given better results as compared to pure WS₂ [53]. The calculated specific capacitance was 383.6 F g⁻¹ at the current density of 0.5 A/g¹.

Table 2.2: Electrochemical properties of various WS₂ based electrode materials.

Electrode	Electrolyte	Specific capacitance	Cyclic stability	Reference
Hierarchical architecture of Graphene /WS ₂	1 M H ₂ SO ₄	383.6 F g ⁻¹	79.9%.	2019[53]
Graphene /WS ₂ core-sheath fibers	PVA/H ₂ SO ₄ (solid state)	270.36 mF cm ⁻²	75.2% @4000cycles	2021[54]
WS ₂ @PPy heterostructure	1 M H ₂ SO ₄	245 F/g	99.2 % at a @20 A/g after 10,000 cycles	2023[55]
WS ₂ nanoflowers	6 M KOH aqueous electrolyte	119 F/g @1A/g		

2.3 ZnCo₂O₄ based supercapacitors.

Binary transition metal oxides are the most researched and investigated compounds as compared to their single metal oxides. Due to the availability of the metal ions and their rich redox chemistry, they have shown good results in the energy storage devices[56]. Among many, ZnCo₂O₄ has unique properties making it suitable for supercapacitors. Numerous research has been performed to find its electrochemical performance. The combination of ZnCo₂O₄ with WS₂ and carbon-based nanomaterials show extraordinary results due to the synergistic effect of each individual constituent.

Table 2.3: Electrochemical properties of ZnCo₂O₄ and its composites

Electrode	Electrolyte	Specific capacitance/capacity	Cyclic stability	Reference
ZnCo ₂ O ₄ Flower of thin nanosheets	1 M KOH	583F/g @10mV/s	96.50%	2021 [57]
ZnCo ₂ O ₄ thin films	6 M KOH	127.8 F/g at 1mA/cm ²	80.66% after 3000	2019[58]
ZnCo ₂ O ₄ mesoporous necklace	2M KOH	439.6 F/g @1A/g	84.82 % after 5000 cycles 40A/g	2021[59]
Mesoporous /urchin like ZnCo ₂ O ₄	6-M KOH	f 72 mAh g ⁻¹ at 5mVs ⁻¹ , 24 mAh g ⁻¹ at .5A/g	97% after 3000 cycles @0.5A/g	2022[60]
ZnWO ₄ /ZnCo ₂ O ₄ nanocomposite		180.121 mA h g ⁻¹	97.83% after 4000 cycles	2023[61]
ZnCo ₂ O ₄ RGO composite		738 at 2 A g	100% after 2000 cycles	2023[61]
petal-like nanoflower WS ₂ / ZnCo ₂ O ₄	3 M KOH	154.74 mA h/g at 5A/g	f 96.34% after 4000 cycles.	2021[41]

CHAPTER 3: MATERIALS AND METHODS

In this research, we prepared a series of materials to investigate their potential for supercapacitor applications. I synthesized ZnCo_2O_4 and WS_2 individually and developed a binary composite of ZnCo_2O_4 and WS_2 . Additionally, I created a composite of ZnCo_2O_4 and COOH-functionalized carbon nanotubes (COOH-CNTs), as well as a ternary composite combining ZnCo_2O_4 , WS_2 , and COOH-CNTs.

These materials were characterized by using X-ray diffraction (XRD) to determine phase purity, scanning electron microscopy (SEM) and energy-dispersive X-ray spectroscopy (EDX) for morphology and elemental composition, BET for surface area and porosity measurement and Fourier-transform infrared spectroscopy (FTIR) for functional group analysis.

Electrochemical performance was assessed for each material, focusing on specific capacitance, rate capability, and cycling stability, to compare their effectiveness as supercapacitor electrodes and evaluate the benefits of the ternary composite over the others.

3.1 Design of Experiment

This work focuses on the individual synthesis and characterization of ZnCo_2O_4 , WS_2 and FCNTs followed by their electrochemical testing. ZnCo_2O_4 can be synthesized by various routes, but hydrothermal synthesis is the easy and better way to synthesize ZnCo_2O_4 [41, 62, 63]. Liquid phase exfoliation method was used to synthesize WS_2 [53, 64], while COOH-FCNTs were purchased. Binary composites of ZnCo_2O_4 and WS_2 were made again by hydrothermal method.

Also, the same method was followed for the composite's synthesis of ZnCo_2O_4 and FCNTs. Literature lacks the synthesis process for the synthesis ternary composite of all the three. There is no work reported on the ternary composite of ZnCo_2O_4 , WS_2 and FCNTs. (Figure 3.1) shows the general experimental design for this work. Synthesis of each material is explained below in detail.

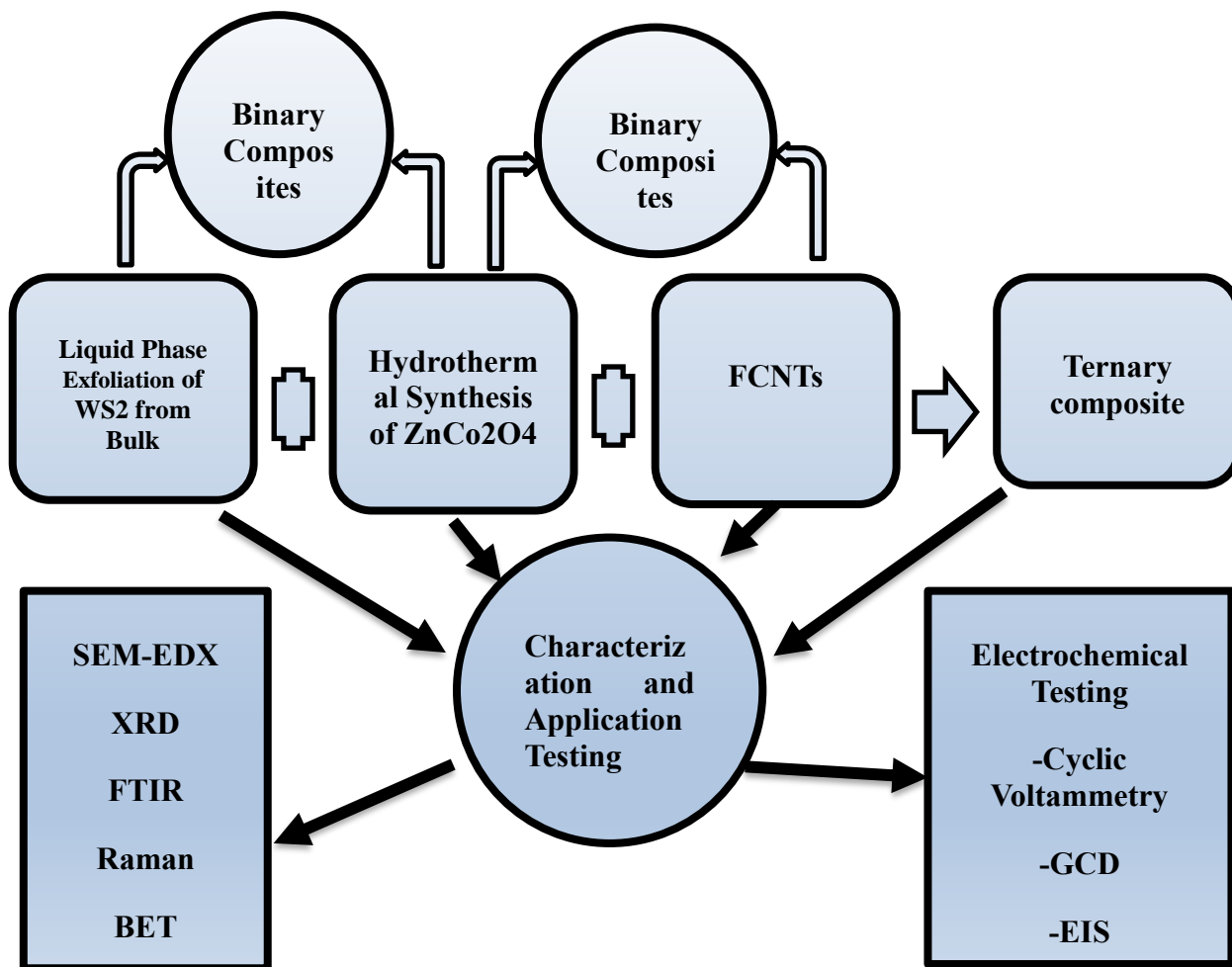


Figure 3.1. Schematic illustration of the design of experiment.

3.2 Synthesis of ZnCo_2O_4

Hydrothermal method was opted for the synthesis of ZnCo_2O_4 .

3.2.1 Materials Required

1. Zinc nitrate hexahydrate
2. Cobalt nitrate hexahydrate
3. Urea
4. Ammonium fluoride

5. Deionized water

3.2.2 Apparatus

1. Hot plates with magnetic stirrer
2. Oven
3. Autoclave
4. Furnace
5. Centrifuge
6. Beakers
7. Petri dishes
8. Weighing balance
9. Fume hood

3.2.3 Synthesis

4 mmol of $\text{Co}(\text{NO}_3)_2 \cdot 6\text{H}_2\text{O}$, 2 mmol of $\text{Zn}(\text{NO}_3)_2 \cdot 6\text{H}_2\text{O}$, 9 mmol of urea and 2 mmol of NH_4F were dissolved in 50 ml of Deionized water and stirred for 30 minutes. The solution was then transferred to a 100 ml Teflon lined autoclave. Hydrothermal reaction at 180°C was carried out for 10 hours. The sample was washed with DI water three times followed by washing with ethanol 3 times. The sample was dried at 100°C .

Finally, the samples were annealed at 200°C , 300°C , 400°C and 500°C for 5hrs at the ramp rate of $2^\circ\text{C}/\text{min}$ [60]. Results of representative sample are discussed in the results and discussion section.

The obtained samples were characterized by SEM, XRD, FTIR, Raman spectroscopy followed by application testing.

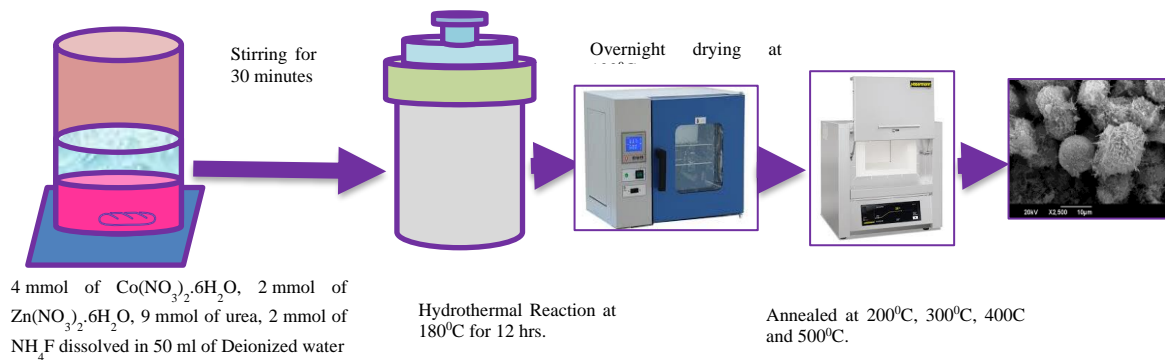


Figure 3.2: Hydrothermal synthesis of ZnCo_2O_4

3.3 Synthesis of WS_2

Liquid phase exfoliation method was opted for the synthesis of WS_2 .

3.3.1 Materials Required

1. Bulk WS_2
2. NMP
3. DI Water
4. Ethanol

3.3.2 Apparatus

1. Hot plates with magnetic stirrer
2. Oven
3. Centrifuge
4. Probe sonicator
5. Beakers
6. Petri dishes

7. Weighing balance

8. Fume hood

3.3.3 Synthesis

(JY91-IIN N&DN Series) used for ultrasonication. 2 grams of bulk WS_2 (Sigma Aldrich 99.9%) was dissolved in 80 ml of NMP (>99.5%) and ultrasonicated with an output power of 650W for 1 hour. The solution was then transferred to a stainless-steel beaker and placed in a probe sonicator. The power and frequency set were 600W and 25kHz respectively, and the sonication was done for 8 hours at room temperature [65, 66].

Then the dispersed solution was centrifuged (Model etc) for 20 minutes at 1000, 2000, 3000 and 4000 RPM. The supernatant was vacuum filtered using nylon filter papers with 0.45 micron pore size. The Obtained nanosheets were oven dried at $80^{\circ}C$ for 12 hours. This process was repeated many times to obtain a reasonable yield. Synthesized nanosheets were characterized by XRD, and FTIR [65-68].

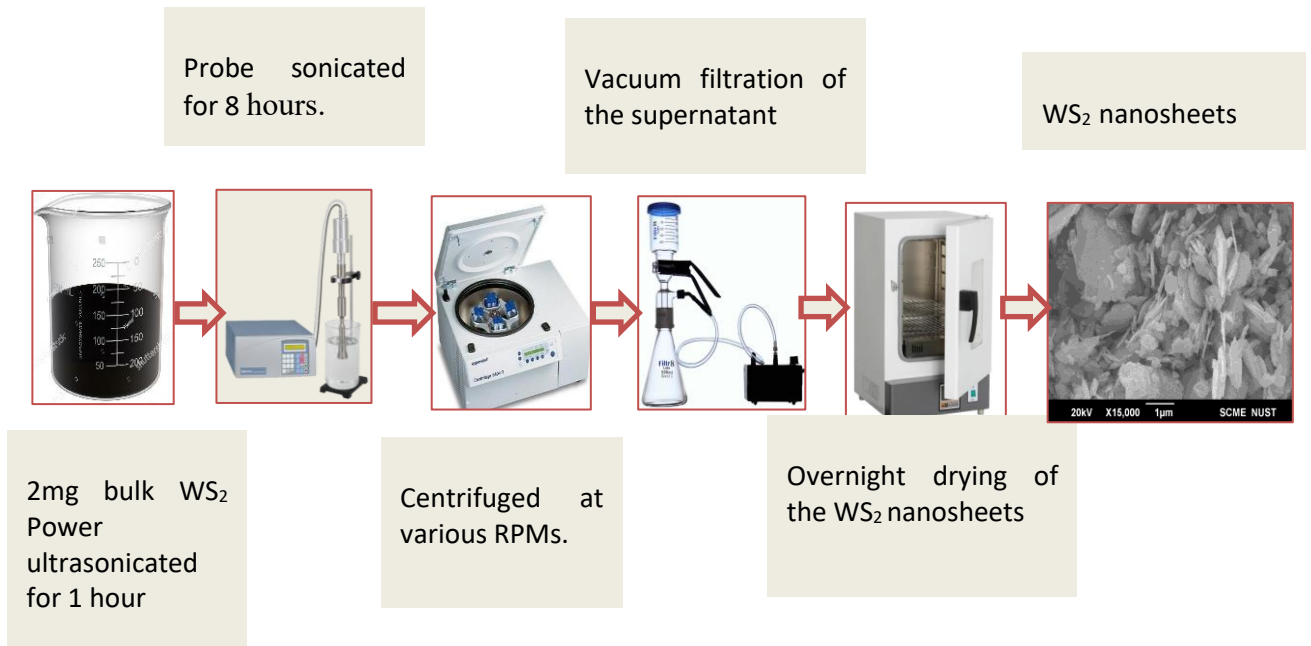


Figure 3.3: Schematics of synthesis of WS_2 nanosheets through liquid phase exfoliation

3.4 Synthesis of ZnCo₂O₄/WS₂ Composite

4 mmol of Co(NO₃)₂.6H₂O, 2 mmol of Zn(NO₃)₂.6H₂O, 9 mmol of urea and 2 mmol of NH₄F were dissolved in 50 ml of Deionized water and stirred for 30 minutes. 0.2grams of WS₂ nanosheets were added to the solution and ultrasonicated for 30 minutes. Then the solution was transferred to a 100 ml Teflon cylinder and kept in autoclave at 180⁰C for 5 hours. The samples were washed with DI water and absolute ethanol 3 times respectively. The sample was dried at 80⁰C overnight followed by annealing at 100⁰C, 200⁰C and 300⁰C respectively. The best sample was taken and discussed in results and discussion portion.

3.5 Synthesis of ZnCo₂O₄/FCNTs Composite

4 mmol of Co(NO₃)₂.6H₂O, 2 mmol of Zn(NO₃)₂.6H₂O, 9 mmol of urea and 2 mmol of NH₄F were dissolved in 50 ml of Deionized water and stirred for 30 minutes. Then 0.2mg of FCNTs were added to the mixture and again stirred for 30 minutes.

The solution was then transferred to a 100 ml Teflon lined autoclave and kept in oven at 180⁰C for 5 hours. The sample was washed with DI water and absolute ethanol subsequently and dried at 80⁰C for 12 hours. Then it was calcined for 5 hours at 300⁰C. the ramp rate was set to 2⁰C/min

3.6 Synthesis of ZnCo₂O₄/WS₂/FCNTs Composite

Hydrothermal method was opted for the synthesis of ZnCo₂O₄.

3.6.1 *Materials Required*

1. Zinc nitrate hexahydrate
2. Cobalt nitrate hexahydrate
3. Urea
4. Ammonium fluoride
5. WS₂ nanosheets
6. FCNTs

7. Deionized water

3.6.2 Apparatus

1. Hot plates with magnetic stirrer
2. Oven
3. Autoclave
4. Furnace
5. Centrifuge
6. Beakers
7. Petri dishes
8. Weighing balance
9. Fume hood

3.6.3 Synthesis

0.2M (3.5688grams) $\text{Zn}(\text{NO}_3)_2 \cdot 6\text{H}_2\text{O}$, 0.4M (6.9847grams) $\text{Co}(\text{NO}_3)_2 \cdot 6\text{H}_2\text{O}$, 0.9M urea and 0.2M NH_4F were added in a 60ml distilled water and stirred for 30 minutes. 0.2688 grams WS_2 and 0.02290 grams of FCNTs were added to the solution during stirring and kept it for another 30 minutes.

The solution was then transferred to a 100ml Teflon lined autoclave and hydrothermal reaction was carried out at 150°C for 5 hours. The sample was washed thrice with Distilled water and absolute ethanol respectively.

The sample was dried overnight at 100°C . Then it was calcined at 350°C for 5 hours with a ramp rate of $2^\circ\text{C}/\text{min}$ [60]. Figure 3.4 shows the schematics of the synthesis of ternary composite.

3.7 Characterization Techniques and sample preparations

The characterization techniques used were X-Ray Diffraction (Brooker, D2 Phaser), Scanning Electron Microscopy (JASM-6490A, Jeol Japan), and Energy Dispersive Xray Spectroscopy (EDAX, AMETEK), BET surface area and porosity analyzer (Gemini VII 2390 V1.03 (V1.03 t) of Micromeritics instrument corp.) and Fourier Transform Infrared Spectroscopy (Perkin Elmer, USA, Spectrum 100)

Powder samples analyzed in XRD within the scan angle of 2θ 10° to 90° . The samples were homogenized using mortar and pestle and then heated in an oven at 60°C to avoid any adsorbed water. The samples were then placed in XRD sample holders and pressed to the powder using a glass slide.

The SEM and EDX analysis were done using powder samples. The samples were grind using a mortar and pestle. Carbon double side tape was used to stick a few of the powder samples on to the metallic (Steel/Cu) stubs. The samples were then sputtered gold coated using argon as an ionizing gas. The coating thickness set was set to 30 nm. The samples were placed in the SEM sample holder and placed in a low vacuum SEM. The accelerating voltage was 20kV and a working distance of 10mm was maintained during the imaging. Secondary electron detector was used for imaging and EDX detector was used to find the elemental composition.

The BET surface area and porosity was done using N_2 adsorption. The sample was degassed at 100°C for 2 hours. To prepare a sample for Fourier-Transform Infrared (FTIR) spectroscopy using potassium bromide (KBr) pellets, grinded both the sample and KBR powder finely. Mixed 1-2 mg of sample to 100 mg of KBr. Transferred the mixture into a die and pressed it using a hydraulic press of 10 tons load. Placed the pallet in the FIR sample holder. Initially record the background spectrum using a neat KBr pallet, and then measured the sample spectrum withing the range of 300 to 4000 cm^{-1} . The results were then plotted and analyzed.

3.8 Samples Preparation for Electrochemical Testing

The electrochemical measurements were taken using three electrode system of (Gamry, INTERFACE1010E). Samples were prepared by mixing of 8mg of active material in 5ml

absolute ethanol and 5wt% Nafion solution. The mixture was ultrasonicated for 40 mins to form an ink. The dispersed ink was then dropped on the 1x1 cm² activated Nickel Foam and kept for drying in an oven. The solution was again kept for sonication.

This process was repeated by changing the side of Ni Foam until at least 2mg active materials was coated. Then the samples were kept in a vacuum oven for 24 hrs at 60⁰C. The prepared samples were taken as working electrodes, Ag/AgCl as reference electrode and platinum wire as counter electrode. The operating window was set between -0.4V to 0.8 V in 3M KCL electrolyte. Cyclic voltammetry was run at different scan rates ranging from 5mV/s to 100mV/s. The specific capacitance was calculated using the equation:

$$C = \frac{A}{2m\Delta V.V}$$

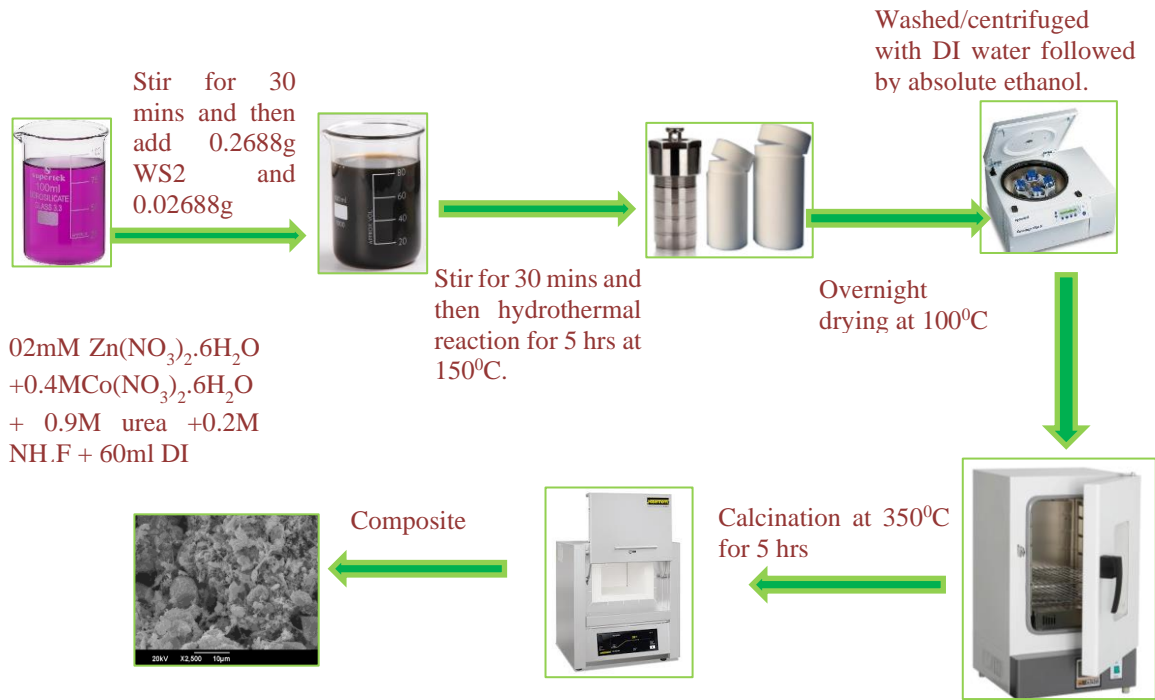


Figure 3.4: Schematics of synthesis of ZnCo₂O₄/WS₂/FCNTs composite

Where C is specific capacitance (F/g), A is area under the graph of CV plot, m is the mass of the active material (g), ΔV is the potential window(V) and V is the scan rate (V/s). Electrochemical impedance spectroscopy (EIS) was done in the frequency range of

100 mHz to 100 kHz and GCD was done at the current densities of 0.5Ag^{-1} , 15Ag^{-1} , 25Ag^{-1} and 55Ag^{-1} .

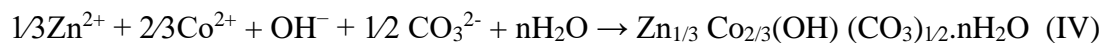
CHAPTER 4: RESULTS AND DISCUSSION

Following characterization techniques were used to characterize the synthesized materials.

- SEM/EDX
- XRD
- BET surface area and porosity analyzer.
- FTIR
- Electrochemical testing

4.1 SEM Analysis

SEM results of all the representative samples of each set are shown in Fig.4.1. The images of ZnCo_2O_4 at various magnifications are shown in Fig.4.1a-c. which show mixed morphology of flower-like structures with porous surfaces and urchin-like structures with nanowires[60]. The nucleation of nanowire with nanoflakes is due to the addition of urea in the synthesis[69]. Initially the urea decomposes into CO_3^{2-} and OH^- metal complexes are formed once the anions combine with Zn and Co hydroxides, thus forming many nucleation centers. Based on the interfacial energy, the nuclei grow and auto assemble. The interfacial energy is dependent on the type of surfactant used. Urea produces nanowires which further grow into spheres of urchin-like structure upon annealing or calcination. [60, 69, 70]. The reaction involved in the formation of ZnCO_2O_4 are given below.



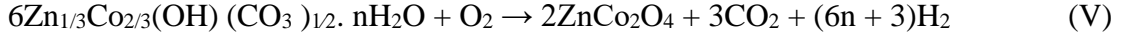


Fig.4.1d is the SEM image of COOH functionalized CNTs. The surface morphology is rough and dense because of the addition of the carboxyl group [19, 71, 72]. Fig.4.1e-f are SEM images of bulk WS₂ and WS₂ nanosheets respectively which clearly indicate that the bulk WS₂ has been exfoliated to thin and small sheets. The lateral dimensions are in few micrometers while the thickness is in the range of 60 to 90 nm.

Fig.4.1g-h are the SEM images of ZnCO₂O₄/WS₂. It is clearly seen that the WS₂ nano sheets have been incorporated into the matrix of ZnCO₂O₄. The morphology of ZnCO₂O₄ has changed from flower-like structure to ball-like structure. Figure.4.1i, is SEM image of ZnCO₂O₄/FCNTs showing a morphology of deformed spheres of ZnCO₂O₄ in combination with FCNTs. Fig.4.1j-l are the morphology of ZnCO₂O₄/WS₂/FCNTs.

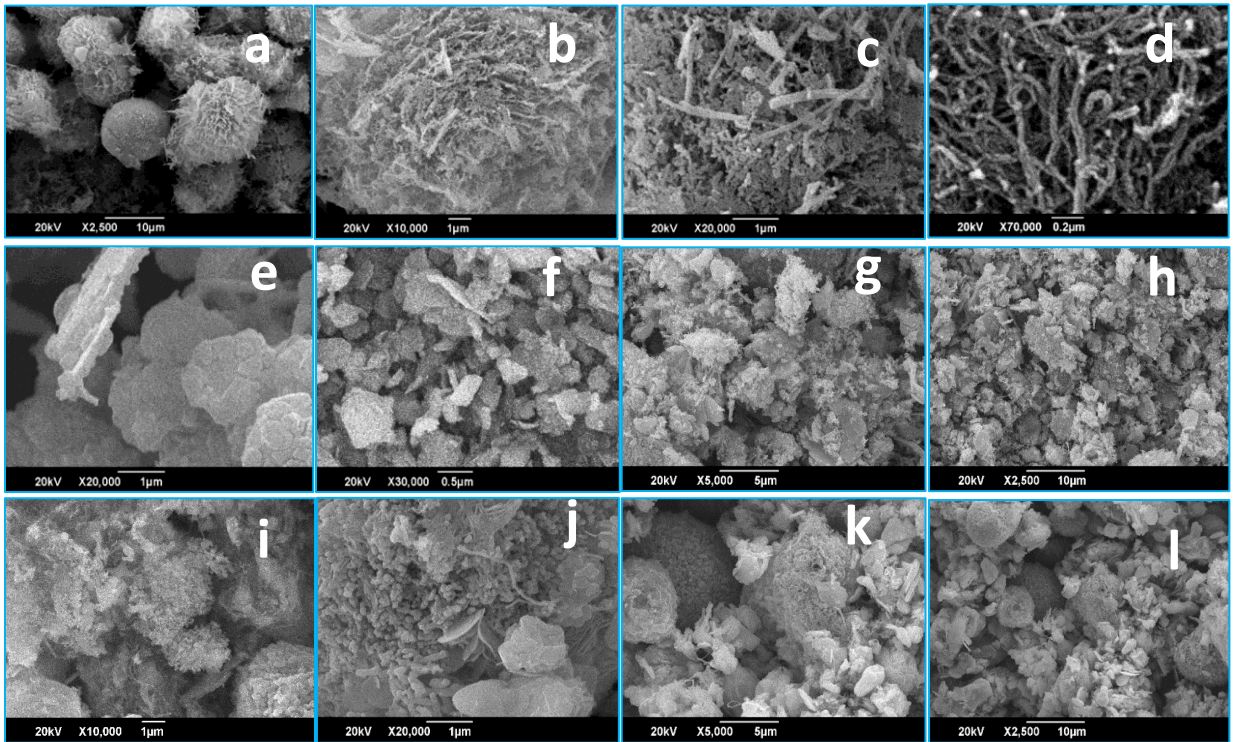


Figure 4.1: SEM results of (a-c) ZnCO₂O₄, (d) FCNTs, (e & f) bulk WS₂ and WS₂ nanosheets, (g & h) ZnCO₂O₄/WS₂, (i) ZnCO₂O₄/FCNTs & (j-l) ZnCO₂O₄/WS₂/FCNTs

The SEM images show that the composite has a mesoporous ZnCO_2O_4 particles, WS_2 nanosheets and Functionalized CNTs which indicates that the composite has been formed successfully. The ZnCO_2O_4 morphology lacks nanowire like structures in the ternary compounds, showing a bunch of particles on surface at high magnification(j). It is evident from the micrographs that WS_2 and FCNTs have been incorporated successfully.

4.2 Energy Dispersive X-Ray Spectroscopy

Energy dispersive X-ray spectroscopy was done to find the elemental composition and mapping of the prepared samples. Results are discussed below.

4.2.1 EDX results of COOH Functionalized CNTs

Figure 4.2 shows the SEM images with a selected area on the left side and the corresponding EDX spectrum and compositional table on right side for the functionalized carbon nanotubes. The atomic and weight percentages of carbon are 89.5 % and 86.5 % respectively, while that of Oxygen are 105 and 13.5 % respectively. As the carbon nanotubes are primarily composed of carbon, so the high percentage of carbon is associated with CNTs, while the presence of oxygen is associated with COOH group, which indicates that the CNTs have been functionalized successfully.

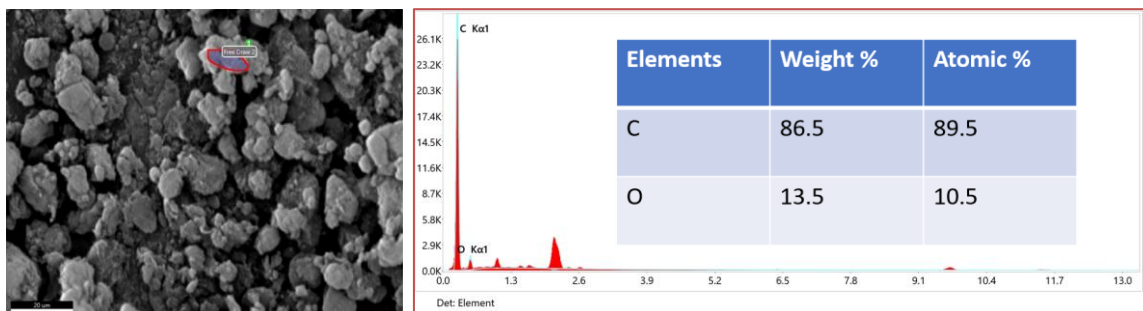


Figure 4.2: EDX spectrum and the composition table of COOH-Functionalized CNTs

EDX Results of WS_2 nanosheets are presented in figure 4.3. The characteristic peaks of Tungsten and Sulfur have been detected in EDX spectrum. Moreover, the atomic percentages of W and S are 33.8% and 66.2%

respectively. The atomic percentages show the exact stoichiometric ratio of W and S which is 1 ratio 2. The higher weight percentage of tungsten (74.5%) is due to its higher atomic mass as compared to the sulfur.

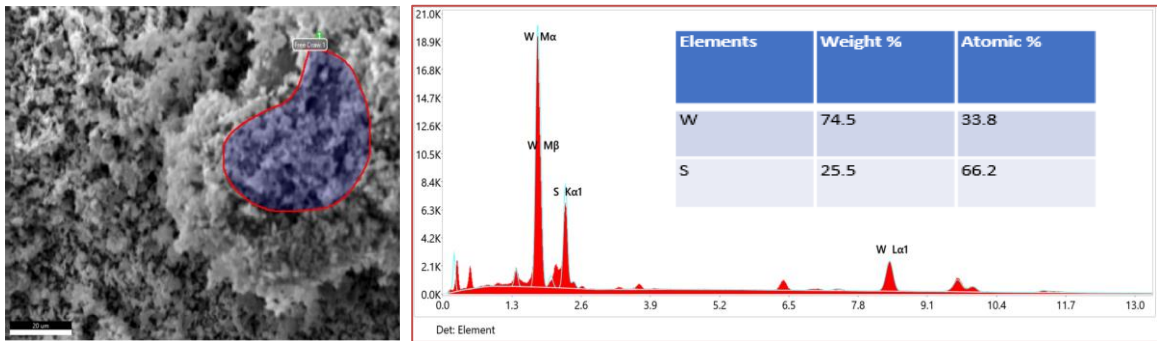


Figure 4.3: EDX spectrum and the composition table of WS₂ Nanosheets

Figure 4.4 represents the EDX results of ZnCo₂O₄ which confirms the presence of all the three elements of ZnCo₂O₄. The atomic percentages of the Zn, Co and Oxygen are inconsistent with the stoichiometric ratios of ZnCo₂O₄ which is 1:2:4. This confirms the successful synthesis of ZnCo₂O₄. The weight percentage of cobalt is higher (51.4%) as its atomic mass is greater than Zn and Oxygen. Oxygen, being the lightest element has the lowest weight percentage i.e., 21%.

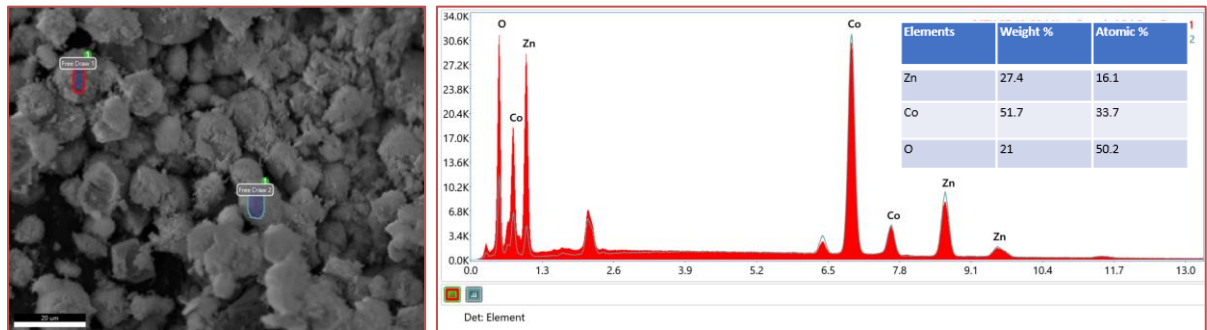


Figure 4.4: EDX spectrum and the composition table of ZnCo₂O₄

Figure 4.5 shows the Elemental mapping along with the composition table and EDX spectrum. The elemental mapping confirms the distribution of Zn, Co, O and C. The bright regions on carbon map indicate the heterogeneous distribution, but the degree of

heterogeneity is very less. The atomic percentages of the Zn, Co and O are inconsistent with the empirical formula of $ZnCo_2O_4$ which is 1:2:4. The atomic percentage of carbon is 29.9% which contributes a weight percentage of 12.3% of the of the composite.

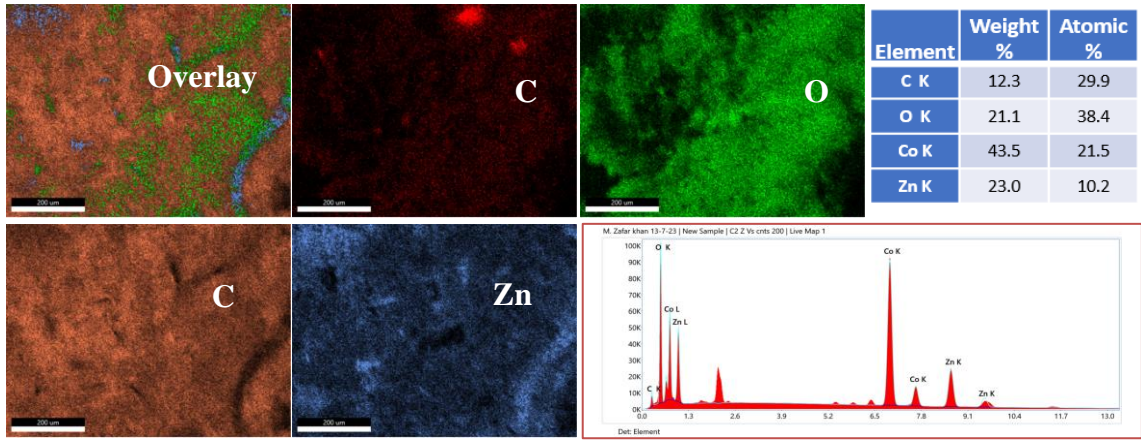


Figure 4.5: Elemental Mapping composition table and EDX spectrum of binary composite $ZnCo_2O_4/FCNTS$

The atomic percentages of Zn, Co and O are 23%, 43.5 and 21.1 % respectively, which make a total 87.6 weight % of $ZnCo_2O_4$. It confirms a successful development of a binary composite $ZnCo_2O_4/FCNTs$ with an overall weight percentage of 87.6% $ZnCo_2O_4$ and 12.4% C.

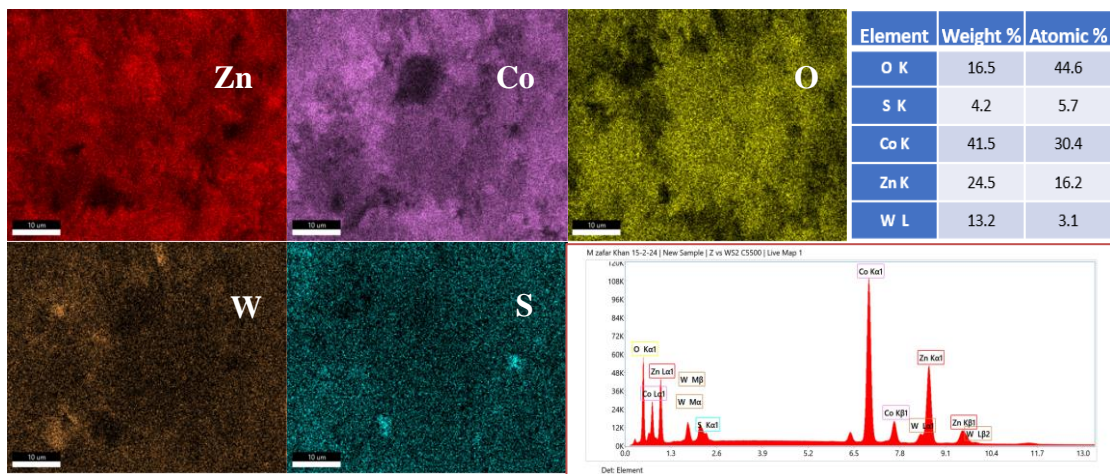


Figure 4.6: Elemental Mapping composition table and EDX spectrum of binary composite $ZnCo_2O_4/WS_2$.

The EDX spectrum and mapping results in figure 4.6 provide the information regarding the elemental composition and distribution of the binary composite $\text{ZnCO}_2\text{O}_4/\text{WS}_2$. The EDX spectrum contains all the characteristic peaks of all the elements present (Zn, CO, O, W, S). The atomic percentages are inconsistent with the stoichiometry of ZnCO_2O_4 and WS_2 .

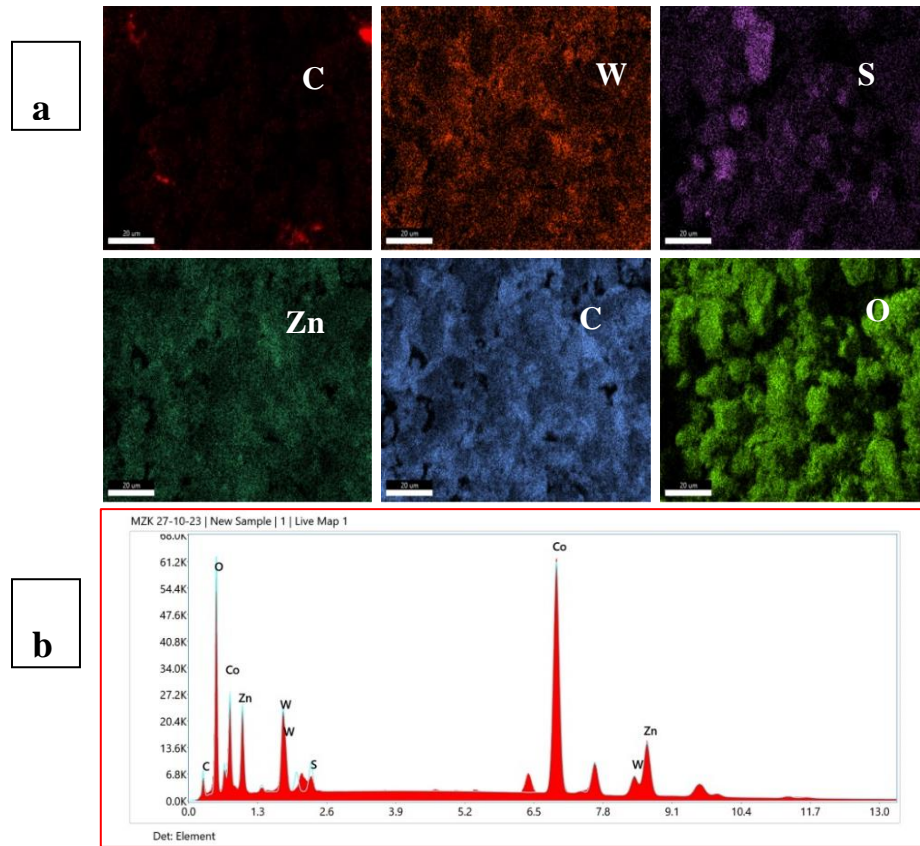


Figure 4.7: a) Elemental Mapping of $\text{ZnCO}_2\text{O}_4/\text{WS}_2/\text{FCNTs}$ and b) EDX spectrum of $\text{ZnCO}_2\text{O}_4/\text{WS}_2/\text{FCNTs}$

Elemental mapping of the ternary composite was done to visualize the distribution of all the elements. Fig.5a-b presents the elemental mapping data and EDX spectra of the ternary composite $\text{ZnCO}_2\text{O}_4/\text{WS}_2/\text{FCNTs}$. It is clearly seen that all the elements (Zn, Co, O, C, W, S) are present. The red colored map of carbon shows that it is almost distributed homogeneously, with some intense areas or patches showing larger amounts of carbon. The map of Tungsten and sulfur shows that they are distributed homogeneously confirming the formation of WS_2 . There are few patches which are rich in W and S, but both the W

and S rich areas are same, which means W and S exist together forming WS₂. The map of Co is almost double intense as Zn confirming the stoichiometric ratio, both the maps are replicas of each other. Moreover, the O map is more intense as oxygen is 4 times of Zn and double of Co. Oxygen from the carboxyl group of FCNTs also adds up to the intensity of the O map and to the atomic ratio and weight percentage.

4.3 BET Results

The BET specific surface measurements of WS₂, ZnCO₂O₄, FCNTs and ZnCO₂O₄/WS₂/FCNTs were done to find the Specific surface area, average pore width and pore volume. Table 4.1 shows the results of BET surface area, average BJH pore width and average volume. The BET Specific Surface Area (SSA), single point surface area at ($p/p^\circ = 0.244382477$) and the Langmuir Surface Area of the WS₂ nanosheets are 26.0846 m²/g, 25.8223 m²/g and 27.0075 m²/g respectively which are the lowest among all the samples. The surface area of FCNTs is 35.9185 m²/g and that of ZnCO₂O₄ is 63.1742 m²/g.

Table 4.1: BET surface area, pore width and pore volume values

Name	BET Surface area m ² /g	Average Pore Width (nm)	BJH cumulative Pore Volume (cm ³ /g)
ZnCO ₂ O ₄ /WS ₂ /FCNTs	218.3964	10.6456	0.677564
ZnCO ₂ O	63.1742	4.5515	0.046113
FCNTs	35.9185	3.2558	0.028525
WS ₂	26.0846	5.9284	0.041742

The adsorption isotherm and the pore distribution of the ternary composite is shown in figure 4.8. The adsorption curve resembles type-IV suggesting the mesoporous nature of the composite. The BET surface area of the ternary is calculated to be 218.3964m²/g, and the BJH adsorption average pore size of ZnCO₂O₄/WS₂/FCNTs 10.6456nm. The total area in pores with size greater than 15.9nm is 12.911 m²/g, total area in pores with size

smaller than 1.483nm is 124.113 m²/g and the area in pores with size in between 1.148-15.9nm is 81.156 m²/g. The SSA of the ternary composites is very high as compared to the individual constituents. This good porosity and high specific surface area can lead to enhanced electroactive sites, and the highest pore volume ensures fast ion transport and easier electrolyte accessibility, ultimately resulting in an improved electrochemical property. Moreover, the average pore width confirms the mesoporous nature of the synthesized composite.

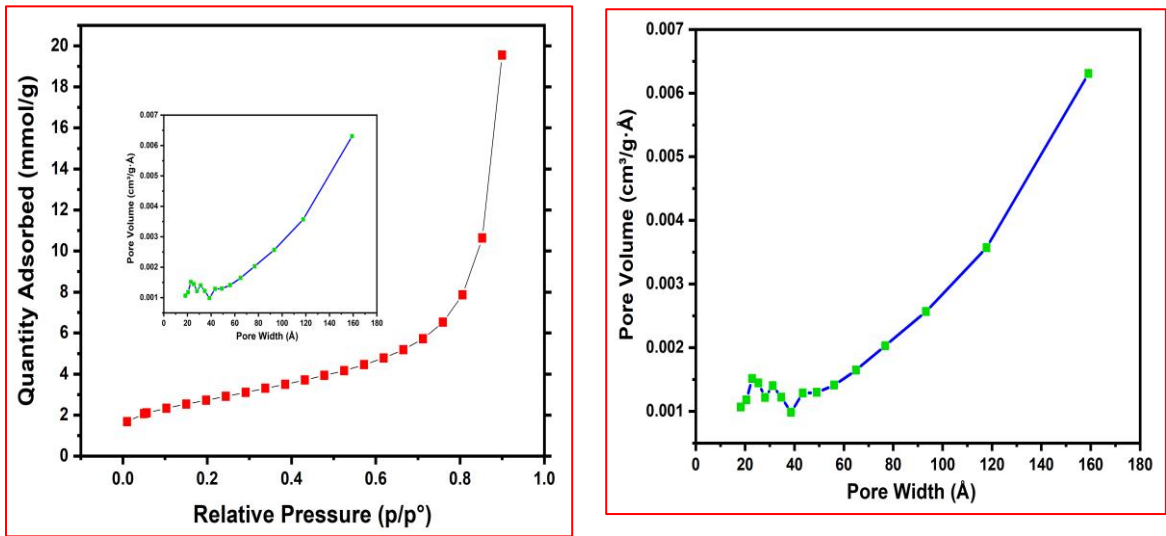


Figure 4.8: The adsorption isotherm and the pore distribution of the ternary composite ZnCO₂O₄/WS₂/FCNTs

4.4 X-Ray Diffraction Results

X-Ray Diffraction (Brooker, D2 Phaser) was used to study the crystal structure of the synthesized materials. Fig.4.9 shows the XRD plots of all the samples. The three peaks that correspond to the MWCNT-COOH are (100), corresponds to (101) and (004) plane.

XRD spectrums of WS₂ show that the bulk WS₂ has an intense peak at 14.3⁰ corresponding to (002) plane and peaks at 28.9⁰, 32.8⁰, 33.6⁰, 39.5⁰ and 43.9⁰ were assigned to (004), (100), (101), (103) and (106) of hexagonal 2H WS₂ (pdf # 08-0237).

The exfoliated WS₂ has a less intense peak at 14.3⁰ and rest of the peaks disappeared which indicates the decrease in the crystallinity and formation of nanosheets[41, 55, 73, 74].

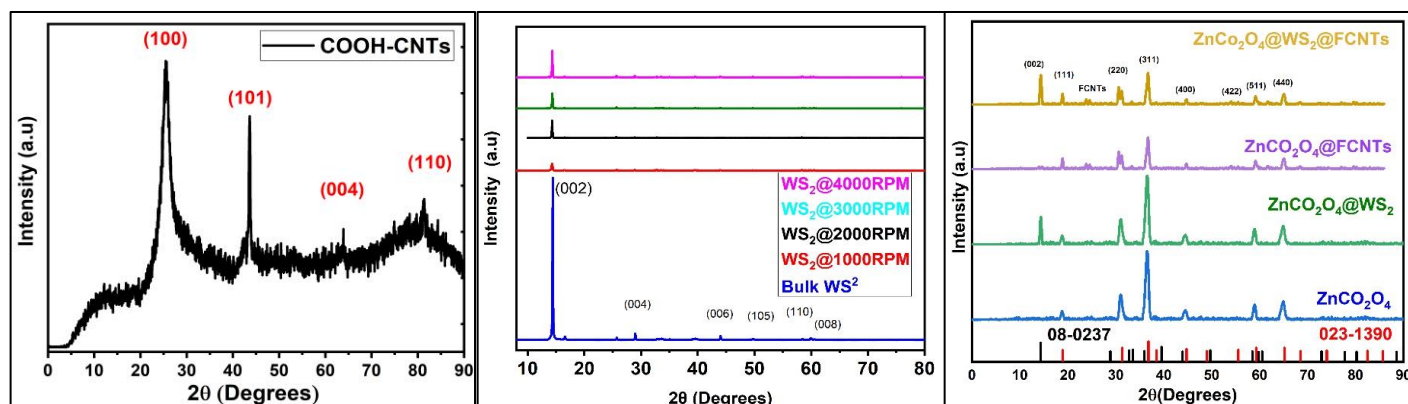


Figure 4.9: XRD spectrum of all the samples

XRD plot of ZnCO_2O_4 matches with pdf # 023-1390. The peaks at 2θ of 18.92° , 31.11° , 36.65° , 38.54° , 44.59° , 59.05° , and 64.85° correspond to the (111), (220), (311), (222), (400), (422), (511), and (440), planes. It confirmed the cubic crystal structure and $Fd\bar{3}m$ space group. Crystallite size found using Sherrer formula is 12.5nm and the average lattice strain is around 0.995% as shown in table 4.2.

Table 4.2: Shows the lattice strain and crystallite size of ZnCO_2O_4 .

No.	B obs. [2θ]	B std. [2θ]	Peak pos. [2θ]	B struct. [2θ]	Crystallite size [\AA]	Lattice strain [%]
1	0.874	0.008	18.702	0.866	93	2.316
2	0.51	0.008	31.069	0.502	164	0.8
3	0.655	0.008	36.58	0.647	129	0.865
4	0.874	0.008	44.46	0.866	99	0.933
5	0.583	0.008	58.929	0.575	159	0.45
6	0.874	0.008	64.866	0.866	109	0.6
Average values					125.5	0.994

The presence of an intense peaks at 14.3° in the XRD plot of $\text{ZnCO}_2\text{O}_4/\text{WS}_2$ confirmed the formation of a binary composite while a broad peak at 24.36° indicates the incorporation of FCNTs into ZnCO_2O_4 and successful formation of a binary composite of ZnCO_2O_4 and FCNTs. Similarly, there is presence of both the peaks of WS_2 (14.3°) and FCNTs (24.36°) in the XRD results of the ternary composite i.e., $\text{ZnCO}_2\text{O}_4/\text{WS}_2/\text{FCNTs}$ while remaining all the peaks belong to ZnCO_2O_4 .

4.5 FTIR Results

Fig.4.10 shows the FTIR spectrum of (a) COOH-FCNTs, (b) ZnCO_2O_4 , (c) WS_2 and (d) $\text{ZnCO}_2\text{O}_4/\text{WS}_2/\text{FCNTs}$. The broad peak in FTIR spectrum of COOH-FCNTs (fig.4.10a) at 3420 cm^{-1} is attributed to the O—H stretching vibration of hydroxyl groups, while the peak at 1740 cm^{-1} corresponds to the carboxylic (C=O) group attached to MWCNTs[72]. The peaks at 2927 cm^{-1} and 2854 cm^{-1} are assigned to the C—H stretching vibration of methylene generated at defect sites on the acid-oxidized MWCNT surface. The peak at 1627 cm^{-1} corresponds to the stretching mode of the C=C double bond, which forms the framework of the carbon nanotube sidewall. The peak at 1400 cm^{-1} is associated with the bending vibration of the hydroxyl group (O-H) in the carboxyl group[19, 71].

Fig.4.10b shows the FTIR spectrum of ZnCO_2O_4 . The characteristic band around 3430 cm^{-1} is attributed to the stretching vibration mode of the H-O-H group, indicating the presence of chemisorbed water molecules. A prominent band of CO_3^{2-} ions at 1634 cm^{-1} and the symmetric vibration of (COO-) at 1390 cm^{-1} were observed. The bands at 652 cm^{-1} and 557 cm^{-1} correspond to the metal-oxygen vibration frequencies of the metal in tetrahedral clearance (Zn-O) and octahedral clearance (Co-O), respectively, indicating the formation of the ZnCO_2O_4 spinel structure[75, 76].

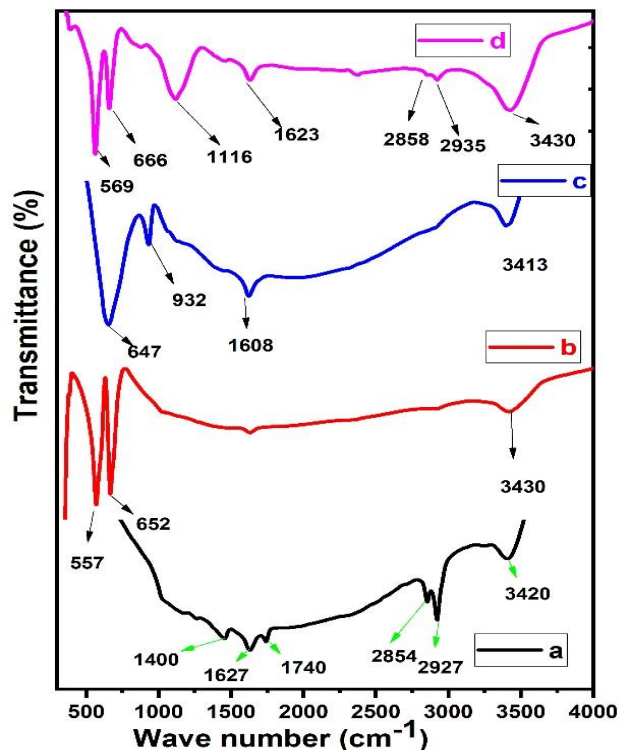


Figure 4.10: FTIR results of (a) COOH-FCNTs, (b) ZnCO₂O₄, (c) WS₂ and (d) ZnCO₂O₄/WS₂/FCNTs

The FTIR spectrum of the WS₂ nanosheets (fig 4.10c) was recorded to analyze the functional groups. The bands at 647 cm⁻¹ and 932 cm⁻¹ correspond to W-S and S-S bonds, respectively. Peaks at 1461 cm⁻¹ and 1645 cm⁻¹ are attributed to the stretching deformation of hydroxyl groups, while those at 2922 cm⁻¹ and 3448 cm⁻¹ are ascribed to OH vibrations[64, 74].

Fig4.10d shows the FTIR spectrum of the ternary composite formed. All the representative peaks of the individual materials are present which indicates the successful formation of the ternary composite. There is an extra peak at 1116cm⁻¹ which can be attributed to the stretching vibrations of metal-oxygen bonds in complex oxide structures.in this case the metal are Zn and Co.

4.6 Application testing results

Application testing of the synthesized electrodes includes cyclic voltammetry, galvanometric charge-discharge, electron impedance spectroscopy and cyclic stability test.

4.6.1 Cyclic voltammetry results

Fig 4.11 shows the Cyclic Voltammetry (CV) curves of the as prepared samples of (a) WS₂, (b) FCNTs, (c) ZnCO₂O₄, (d) ZnCO₂O₄/WS₂, (e)ZnCO₂O₄/FCNTs and (f) ZnCO₂O₄/WS₂/FCNTs at a scan rate of rate of 5, 10, 20 30, 50and 75 mV/s within the potential window of -0.4 to 0.8 V. The electrolyte used was a 3M KOH solution. The CV was done using a reference electrode of Ag/AgCl and platinum as counter electrode. Each material shows an increase in the integral area with increasing scan rate. The CV curves at various scan rates show very strong oxidation and reduction peaks, which indicates the battery nature of the materials.

The increasing trend in the integral area from (a) to (f) indicates that the charge storage capacity increasing from material (a) to (f). Fig 4.13(c) shows the CV plots of all the materials at scan rate of 20mV/s. It is evident that the ternary composite has the highest integral area and redox peak current values. Also, the redox peaks shifted towards more negative and more positive on increasing scan rates. The redox peaks of the composites shifted to both more negative and positive potential regions.

The redox peaks of ZnCO₂O₄/WS₂ (d) are 0.18 and 0.4 volts, that of ZnCO₂O₄/FCNTs (e) are 0.106 and 0.49 volts. The ternary composite has the most negative and positive values which are 0.08 and 0.53 volts. This indicates that the ZnCO₂O₄/WS₂/FCNTs is an electroactive material which provides enough surface and time to interact with electrolyte ions. Moreover, the enhanced redox current and the increasing integral area of the CV curves suggest that the composites synthesized have a greater energy storage capacity. The specific capacitance measured from the CV curves using the formula below are presented in table 4.3.

$$C = \frac{A}{2m\Delta V.V}$$

Where C is specific capacitance (F/g), A is area under the graph of CV plot, m is the mass of the active material (g), ΔV is the potential window(V), and V is the scan rate (V/s).

Table 4.3: shows the specific capacitance at a scan rate of 5mV/s & 20mV/s.

Material	Capacitance (F/g) @ 5mV/s	Capacitance (F/g) @20mV/s
WS ₂	227.53	155.6
COOH-FCNTs	646.29	458.9
ZnCo ₂ O ₄	788.6	708.41
ZnCo ₂ O ₄ /WS ₂	1028.6	907.20
ZnCo ₂ O ₄ /FCNTs	1308.45	1270.6
ZnCo ₂ O ₄ / WS ₂ /FCNTs	1421.93	1386.93

The highest capacitance of the ternary composite is attributed to the synergistic effect of all the three components. The increase in the peak currents indicated that there are more electroactive sites, and more species are available for the redox reactions.

Due to the availability of large number of active sites or surfaces, faster diffusion takes place which increases the electrochemical activity of the electrode.

4.6.2 Galvanometric charge-discharge results

Galvanostatic charge-discharge curves are shown in fig.4.12. The GCD was done at a scan rate of 0.5A/g, 1A/g, 2A/g, and 5 A/g. The lack of linearity in the charge discharge curves indicates the battery nature of the materials.

All the peaks are almost symmetric which means the charge discharge cycles are similar and show good reversibility and efficiency of energy storage. The ternary composite has the highest area under the graph as compared to all other materials which indicates the energy density, and the power density of the ternary composite is higher.

This can be due to the incorporation of FCNTs and WS₂ nanosheets to the ZnCo₂O₄ which increases the conductivity as well as the surface area and active sites. The specific capacitance was calculated using the formula.

$$C = A * \Delta t / \Delta V$$

Where C is the specific capacitance,

A is the current density, Δt is the discharge time and

ΔV is the difference of the potential window.

The specific capacitance at 0.5A/g is presented in table 4.4.

Table 4.4: Specific Capacitance of all the synthesized materials at 0.5A/g

Material	Current Density A/g	Capacitance F/g
WS ₂	0.5	241
COOH-FCNTs	0.5	525
ZnCo ₂ O ₄	0.5	756
ZnCo ₂ O ₄ /WS ₂	0.5	1125
ZnCo ₂ O ₄ /FCNTs	0.5	1210
ZnCo ₂ O ₄ /WS ₂ /FCNTs	0.5	1571

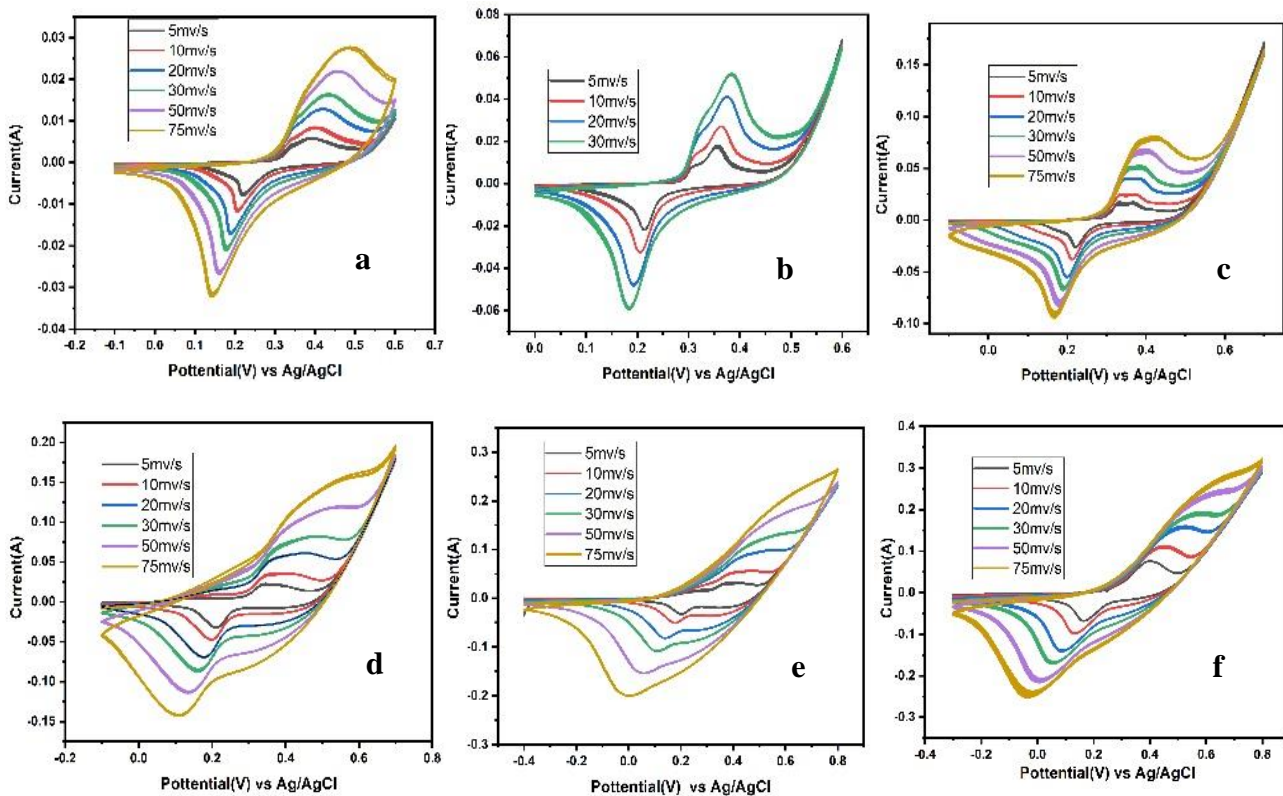


Figure 4.11: CV plots of (a) WS_2 , (b) FCNTs, (c) ZnCo_2O_4 , (d) $\text{ZnCo}_2\text{O}_4/\text{WS}_2$, (e) $\text{ZnCo}_2\text{O}_4/\text{FCNTs}$ and (f) $\text{ZnCO}_2\text{O}_4/\text{WS}_2/\text{FCNTs}$

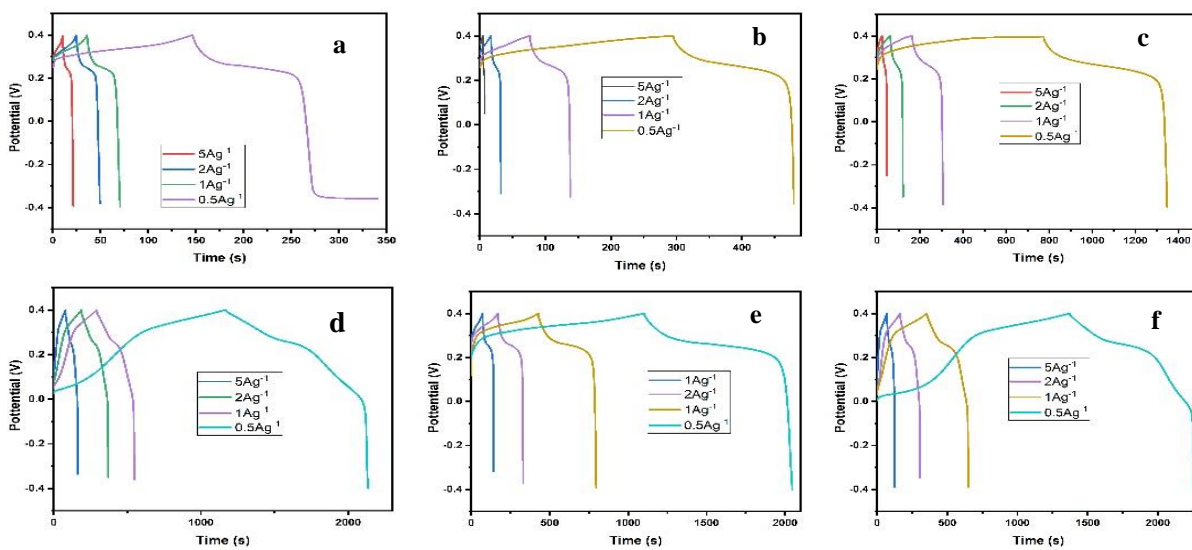


Figure 4.12: GCD plots of (a) WS_2 , (b) FCNTs, (c) ZnCo_2O_4 , (d) $\text{ZnCo}_2\text{O}_4/\text{WS}_2$, (e) $\text{ZnCo}_2\text{O}_4/\text{FCNTs}$ and (f) $\text{ZnCO}_2\text{O}_4/\text{WS}_2/\text{FCNTs}$

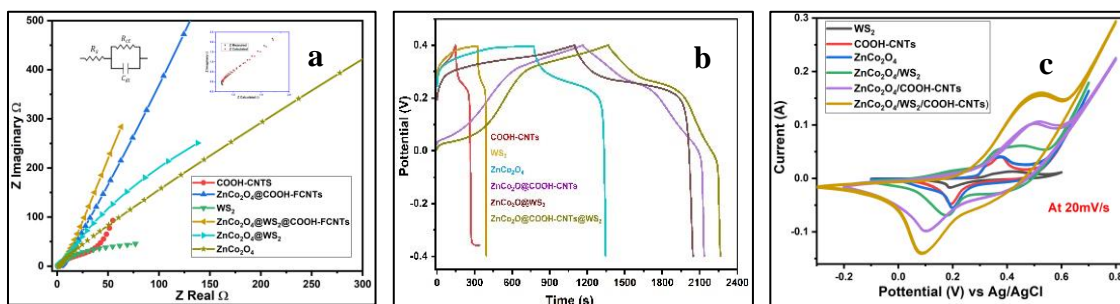


Figure 4.13: (a) CV plots of all samples at 20mV/s, (b) GCD plots of all samples at 0.5A/g and (c) EIS Plots

4.6.3 Electron Impedance Spectroscopy Results

Electron Impedance Spectroscopy (EIS) is used to find out the properties of electrolyte and electrodes. More specifically, Nyquist plot gives information about the electrode and electrode resistance, charge transfer resistance and capacitance.

Figure 4.13(a) represents the Nyquist plots for all the samples. The EIS was done in the frequency range of 100mHz to 100kHz in 3M KOH solutions. The zoomed part of the high frequency region of the ternary composite ZnCO₂O₄/WS₂/FCNTs is also shown matching with Randle's circuit.

A low value of solution resistance R_s was found i.e., 0.804Ω while the R_{ct} value found was 0.78Ω which is due to the vertical semicircle at high frequency region.

The presence of a very small semicircle implies that fast electrochemical reaction takes place. The low internal resistance values indicate that the electrode material has a low conductivity as compared to the others. This leads to less energy loss during charging and discharging.

The straight line in the low frequency region with angle greater than 45° is the evidence of low diffusion resistance, thus exhibiting a fast transport of ions. Based on the electrochemical Properties shown by the ternary composite material, it highly recommended to use as an electrode material for supercapacitor.

4.6.4 Cyclic Stability and Coulombic Efficiency Results

Cyclic stability is a critical parameter for supercapacitors as it indicates how well the device can retain its charge storage capacity over numerous charge-discharge cycles. High cyclic stability is essential for applications requiring long operational lifetimes, such as in electric vehicles, portable electronics, and grid energy storage. The cyclic stability test was done at 10A/g.

The blue plot in figure 4.14 shows the cyclic stability of the ternary composite which basically is the capacity retention of the electrode. It is seen that the capacity retention of the ternary composite is exceptionally good as it shows a 96.6% capacity retention after 5000 cycles and 86.6% capacity retention after 10000 cycles.

Coulombic efficiency is crucial for supercapacitors as it measures the efficiency of charge transfer within the device. High coulombic efficiency means that almost all the charge put into the supercapacitor during charging is recovered during discharging, which is vital for energy-efficient storage and retrieval.

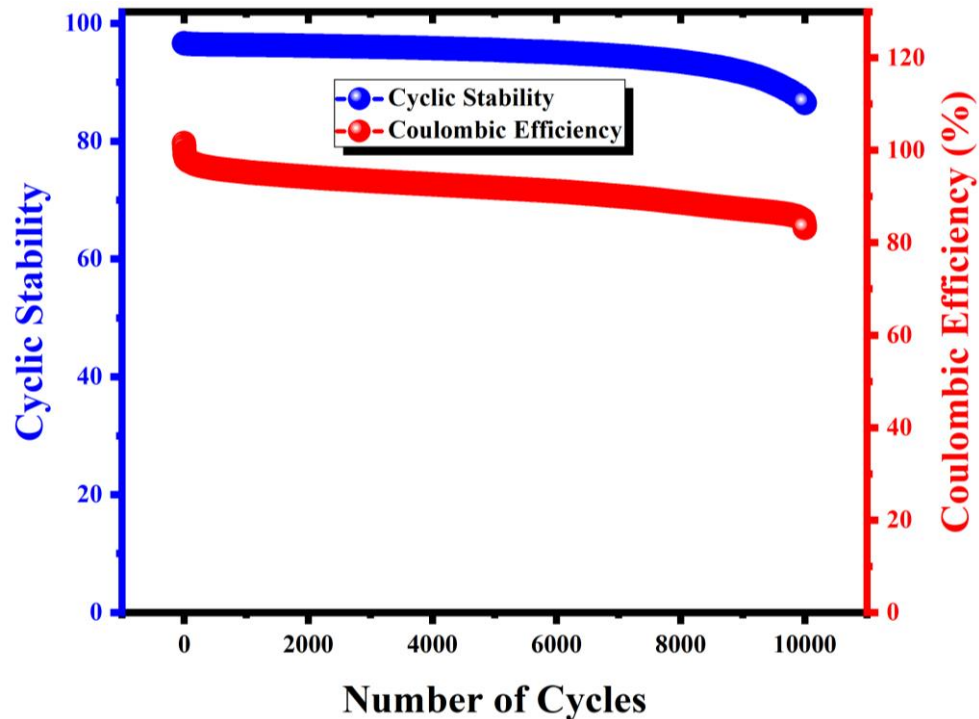


Figure 4.14: Cyclic Stability and Coulombic Efficiency

The red plot in figure 4.14 shows the coulombic efficiency over 10000 cycles. It shows a 91% efficiency for the first 5000 cycles and 85% efficiency was recorded over 10000 cycles. The excellent cyclic stability and high coulombic efficiency observed in the ternary composite of ZnCo_2O_4 , WS_2 , and COOH-CNTs can be attributed to the synergistic effects of these three components. ZnCo_2O_4 offers high theoretical capacity and good electrochemical activity, while WS_2 provides excellent conductivity and structural stability due to its layered structure, which can accommodate volume changes during cycling. COOH-CNTs, on the other hand, enhance the overall electrical conductivity and mechanical strength of the composite, ensuring efficient charge transport and robust structural integrity.

The combination of these materials leads to improved electrochemical performance, where ZnCo_2O_4 's capacity is fully utilized, WS_2 's stability prevents rapid degradation, and COOH-CNTs ensure efficient electron pathways and structural support.

This synergy results in a composite that exhibits remarkable cyclic stability, maintaining nearly 100% capacity over 10,000 cycles, and high coulombic efficiency, with only a slight decline, indicating minimal charge loss and high energy transfer efficiency. Such a performance underscores the potential of this ternary composite for advanced supercapacitor applications, combining high capacity, stability, and efficiency.

CHAPTER 5: CONCLUSIONS AND FUTURE RECOMMENDATION

5.1 Conclusion

Successful synthesis of ZnCo_2O_4 was done using a hydrothermal method, and characterized by using XRD, SEM EDX and FTIR. WS_2 nanosheets were synthesized using a liquid phase exfoliation method from bulk WS_2 and characterized using XRD, SEM EDX and FTIR. Binary composites of $\text{ZnCo}_2\text{O}_4/\text{WS}_2$ and $\text{ZnCo}_2\text{O}_4/\text{FCNTs}$ were successfully synthesized and characterized. Ternary composite of $\text{ZnCo}_2\text{O}_4/\text{WS}_2/\text{FCNTs}$ was synthesized using a simple hydrothermal method. It exhibited a mesoporous morphology consisting of FCNTs, WS_2 nanosheets with spherical porous balls of ZnCo_2O_4 . Fast electrolyte ion transport takes place in such morphology which ultimately enhances the electrochemical properties of the electrode. The specific capacitance calculated from CV curve at a scan rate of 5mV/s is highest for the $\text{ZnCo}_2\text{O}_4/\text{WS}_2/\text{FCNTs}$ (1421.93F/g), followed by $\text{ZnCo}_2\text{O}_4/\text{FCNTs}$ (1308.45F/g), $\text{ZnCo}_2\text{O}_4/\text{WS}_2$ (1028.6F/g), ZnCo_2O_4 (788.6F/g), COOH-FCNTs (646.29F/g) and WS_2 (227.53F/g). The same trend was also observed in the GCD of the electrode.

5.2 Future Recommendations

Research can be done on optimizing synthesis techniques like hydrothermal, sol-gel, chemical vapor deposition etc. Conduct in-depth studies to understand the electrochemical mechanisms and interactions within the composite, focusing on the synergistic effects of ZnCo_2O_4 , WS_2 , and FCNTs. Develop prototype supercapacitors or batteries using the composite material to test real-world performance and scalability.

REFERENCES

- [1] A. T. Hoang, X. P. Nguyen, A. T. Le, T. T. Huynh, and V. V. J. J. o. E. R. T. Pham, "COVID-19 and the global shift progress to clean energy," vol. 143, no. 9, p. 094701, 2021.
- [2] K. M. Tan, T. S. Babu, V. K. Ramachandaramurthy, P. Kasinathan, S. G. Solanki, and S. K. J. J. o. E. S. Raveendran, "Empowering smart grid: A comprehensive review of energy storage technology and application with renewable energy integration," vol. 39, p. 102591, 2021.
- [3] Z. Zhang *et al.*, "A review of technologies and applications on versatile energy storage systems," vol. 148, p. 111263, 2021.
- [4] D. Wang *et al.*, "Energy density issues of flexible energy storage devices," vol. 28, pp. 264-292, 2020.
- [5] J. Mitali, S. Dhinakaran, A. J. E. S. Mohamad, and Saving, "Energy storage systems: A review," vol. 1, no. 3, pp. 166-216, 2022.
- [6] A. Riaz, M. R. Sarker, M. H. M. Saad, and R. J. S. Mohamed, "Review on comparison of different energy storage technologies used in micro-energy harvesting, WSNs, low-cost microelectronic devices: challenges and recommendations," vol. 21, no. 15, p. 5041, 2021.
- [7] A. G. Olabi, M. A. Abdelkareem, T. Wilberforce, E. T. J. R. Sayed, and S. E. Reviews, "Application of graphene in energy storage device—A review," vol. 135, p. 110026, 2021.
- [8] S. S. Siwal, Q. Zhang, N. Devi, and V. K. Thakur, "Carbon-Based Polymer Nanocomposite for High-Performance Energy Storage Applications," *Polymers (Basel)*, vol. 12, no. 3, Feb 26 2020.
- [9] L. Kong, C. Tang, H. J. Peng, J. Q. Huang, and Q. J. S. Zhang, "Advanced energy materials for flexible batteries in energy storage: A review," vol. 1, no. 1, 2020.
- [10] C. V. M. Gopi, R. Vinodh, S. Sambasivam, I. M. Obaidat, and H.-J. J. J. o. e. s. Kim, "Recent progress of advanced energy storage materials for flexible and wearable supercapacitor: From design and development to applications," vol. 27, p. 101035, 2020.
- [11] P. Sinha and K. K. J. H. o. n. s. m. I. P. Kar, "Introduction to supercapacitors," pp. 1-28, 2020.

- [12] A. Dutta, S. Mitra, M. Basak, and T. J. E. S. Banerjee, "A comprehensive review on batteries and supercapacitors: Development and challenges since their inception," vol. 5, no. 1, p. e339, 2023.
- [13] Y. M. J. R. J. o. E. Volkovich, "Electrochemical supercapacitors (a review)," vol. 57, no. 4, pp. 311-347, 2021.
- [14] M. Akin and X. J. I. j. o. e. r. Zhou, "Recent advances in solid-state supercapacitors: From emerging materials to advanced applications," vol. 46, no. 8, pp. 10389-10452, 2022.
- [15] R. Drummond, C. Huang, P. S. Grant, and S. R. Duncan, "Overcoming diffusion limitations in supercapacitors using layered electrodes," *Journal of Power Sources*, vol. 433, p. 126579, 2019.
- [16] P. Sharma and V. J. J. o. E. M. Kumar, "Current technology of supercapacitors: a review," vol. 49, no. 6, pp. 3520-3532, 2020.
- [17] N. I. Jalal, R. I. Ibrahim, and M. K. Oudah, "A review on Supercapacitors: Types and components," in *Journal of Physics: Conference Series*, 2021, vol. 1973, no. 1, p. 012015: IOP Publishing.
- [18] A. G. Olabi, Q. Abbas, A. Al Makky, and M. A. J. E. Abdelkareem, "Supercapacitors as next generation energy storage devices: Properties and applications," vol. 248, p. 123617, 2022.
- [19] H. Sadegh *et al.*, "Synthesis of MWCNT-COOH-Cysteamine composite and its application for dye removal," *Journal of Molecular Liquids*, vol. 215, pp. 221-228, 2016.
- [20] P. Forouzandeh, V. Kumaravel, and S. C. J. C. Pillai, "Electrode materials for supercapacitors: a review of recent advances," vol. 10, no. 9, p. 969, 2020.
- [21] P. Forouzandeh, V. Kumaravel, and S. C. Pillai, "Electrode Materials for Supercapacitors: A Review of Recent Advances," *Catalysts*, vol. 10, no. 9, p. 969, 2020.
- [22] Q. Cheng, J. Tang, N. Shinya, and L.-C. Qin, "Polyaniline modified graphene and carbon nanotube composite electrode for asymmetric supercapacitors of high energy density," *Journal of Power Sources*, vol. 241, pp. 423-428, 2013.
- [23] B. De, S. Banerjee, K. D. Verma, T. Pal, P. Manna, and K. K. J. H. o. N. S. M. I. P. Kar, "Carbon nanotube as electrode materials for supercapacitors," pp. 229-243, 2020.

- [24] T. Wang *et al.*, "Multi-layer hierarchical cellulose nanofibers/carbon nanotubes/vinasse activated carbon composite materials for supercapacitors and electromagnetic interference shielding," vol. 17, no. 3, pp. 904-912, 2024.
- [25] L. Lyu, W. Hooch Antink, Y. S. Kim, C. W. Kim, T. Hyeon, and Y. Piao, "Recent Development of Flexible and Stretchable Supercapacitors Using Transition Metal Compounds as Electrode Materials," *Small*, vol. 17, no. 36, p. e2101974, Sep 2021.
- [26] S. Rani, M. Sharma, D. Verma, A. Ghanghass, R. Bhatia, and I. Sameera, "Two-dimensional transition metal dichalcogenides and their heterostructures: Role of process parameters in top-down and bottom-up synthesis approaches," *Materials Science in Semiconductor Processing*, vol. 139, p. 106313, 2022.
- [27] V. V. Mohan, K. Revathy, C. Adithyan, and R. J. J. o. E. S. Rakhi, "Recent developments of tungsten disulfide-based nanomaterials for supercapacitor applications," vol. 88, p. 111505, 2024.
- [28] O. Öztürk and E. J. C. Gür, "Layered Transition Metal Sulfides for Supercapacitor Applications," p. e202300575, 2024.
- [29] "<fig 1.8Ab_initio_study_of_electronic_and_magnetic_propert.pdf>."
- [30] N. Yousef Tizhoosh, A. Khataee, R. Hassandoost, R. Darvishi Cheshmeh Soltani, and E. Doustkhah, "Ultrasound-engineered synthesis of WS(2)@CeO(2) heterostructure for sonocatalytic degradation of tylosin," *Ultrason Sonochem*, vol. 67, p. 105114, Oct 2020.
- [31] E. Samiei, S. Mohammadi, M. Torkzadeh-Mahani, and M. B. J. B. J. o. P. Askari, "Preparation and characterization of ZnCo2O4 as a binary transitional metal oxide towards pseudocapacitor electrode materials," vol. 51, no. 3, pp. 420-428, 2021.
- [32] S. Kour, S. Tanwar, N. Singh, and A. Sharma, "Electrochemical performance of ZnCo2O4 nanosheets in aqueous electrolytes for supercapacitor applications," in *AIP Conference Proceedings*, 2024, vol. 2995, no. 1: AIP Publishing.
- [34] D. Zhang *et al.*, "Self-assembly of mesoporous ZnCo2O4nanomaterials: density functional theory calculation and flexible all-solid-state energy storage," *Journal of Materials Chemistry A*, vol. 4, no. 2, pp. 568-577, 2016.
- [35] K. V. G. Raghavendra, T. Sreekanth, J. Kim, and K. J. M. L. Yoo, "Novel hydrothermal synthesis of jasmine petal-like nanoflower WS2/ZnCo2O4 as efficient electrode material for high-performance supercapacitors," vol. 285, p. 129133, 2021.

- [36] G. Vignesh *et al.*, "Nitrogen doped reduced graphene oxide/ZnCo₂O₄ nanocomposite electrode for hybrid supercapacitor application," vol. 290, p. 116328, 2023.
- [37] H. Pang, X. Cao, L. Zhu, and M. Zheng, *Synthesis of functional nanomaterials for electrochemical energy storage*. Springer, 2020.
- [38] E. CONVERSION, "ELECTROCHEMICAL ENERGY CONVERSION AND STORAGE SYSTEMS FOR FUTURE SUSTAINABILITY."
- [39] P. K. Sahoo, C.-A. Tseng, Y.-J. Huang, and C.-P. Lee, "Carbon-based nanocomposite materials for high-performance supercapacitors," in *Novel Nanomaterials*: IntechOpen, 2021.
- [40] K. Panchal and D. Kumar, "2D Nanomaterials for Advanced Supercapacitor Application," in *Handbook of Energy Materials*: Springer, 2022, pp. 1-31.
- [41] K. Venkata Guru Raghavendra, T. V. M. Sreekanth, J. Kim, and K. Yoo, "Novel hydrothermal synthesis of jasmine petal-like nanoflower WS₂/ZnCo₂O₄ as efficient electrode material for high-performance supercapacitors," *Materials Letters*, vol. 285, p. 129133, 2021.
- [42] Q. Wang, D. Zhang, G. J. F. S. M. Shen, and Applications, "Flexible Supercapacitors Based on Ternary Metal Oxide (Sulfide, Selenide) Nanostructures," pp. 121-156, 2022.
- [43] J. M. Gonçalves *et al.*, "Recent progress in ZnCo₂O₄ and its composites for energy storage and conversion: a review," *Energy Advances*, vol. 1, no. 11, pp. 793-841, 2022.
- [44] M. Isaacfranklin *et al.*, "ZnCo₂O₄/CNT composite for efficient supercapacitor electrodes," *Ceramics International*, vol. 48, no. 17, pp. 24745-24750, 2022.
- [45] Y. Wang *et al.*, "Synthesis of MOF-74-derived carbon/ZnCo₂O₄ nanoparticles@CNT-nest hybrid material and its application in lithium ion batteries," *Journal of Applied Electrochemistry*, vol. 49, no. 11, pp. 1103-1112, 2019.
- [46] T. Anitha, A. E. Reddy, I. K. Durga, S. S. Rao, H. W. Nam, and H.-J. Kim, "Facile synthesis of ZnWO₄@WS₂ cauliflower-like structures for supercapacitors with enhanced electrochemical performance," *Journal of Electroanalytical Chemistry*, vol. 841, pp. 86-93, 2019.
- [47] K. Aruchamy, A. Balasankar, S. Ramasundaram, and T. H. J. E. Oh, "Recent design and synthesis strategies for high-performance supercapacitors utilizing ZnCo₂O₄-based electrode materials," vol. 16, no. 15, p. 5604, 2023.

- [48] T. Ramachandran and F. Hamed, "Fabrication of dual-1D/2D shaped ZnCo₂O₄ - ZnO electrode material for highly efficient electrochemical supercapacitors," *Journal of Physics and Chemistry of Solids*, vol. 188, p. 111915, 2024.
- [49] R. Dubey, D. Dutta, A. Sarkar, and P. Chattopadhyay, "Functionalized carbon nanotubes: synthesis, properties and applications in water purification, drug delivery, and material and biomedical sciences," *Nanoscale Adv*, vol. 3, no. 20, pp. 5722-5744, Oct 12 2021.
- [50] X. Shang *et al.*, "Carbon fiber cloth supported interwoven WS₂ nanosplates with highly enhanced performances for supercapacitors," *Applied Surface Science*, vol. 392, pp. 708-714, 2017.
- [51] L. Miao, Z. Song, D. Zhu, L. Li, L. Gan, and M. Liu, "Recent advances in carbon-based supercapacitors," *Materials Advances*, vol. 1, no. 5, pp. 945-966, 2020.
- [52] Z. Zhai *et al.*, "A review of carbon materials for supercapacitors," *Materials & Design*, vol. 221, p. 111017, 2022.
- [53] W. Chen, X. Yu, Z. Zhao, S. Ji, and L. Feng, "Hierarchical architecture of coupling graphene and 2D WS₂ for high-performance supercapacitor," *Electrochimica Acta*, vol. 298, pp. 313-320, 2019.
- [54] M. Tang, Y. Wu, J. Yang, H. Wang, T. Lin, and Y. Xue, "Graphene/tungsten disulfide core-sheath fibers: High-performance electrodes for flexible all-solid-state fiber-shaped supercapacitors," *Journal of Alloys and Compounds*, vol. 858, p. 157747, 2021.
- [55] A. De Adhikari, S. Singh, and I. Lahiri, "WS₂@PPy heterostructured high performance supercapacitor self-powered by PVDF piezoelectric separator," *Journal of Alloys and Compounds*, vol. 939, p. 168713, 2023.
- [56] A. Mathivanan, M. Jothibas, and N. Nesakumar, "Synthesis and characterization of ZnCo₂O₄ nanocomposites with enhanced electrochemical features for supercapacitor applications," *Surfaces and Interfaces*, vol. 49, p. 104443, 2024.
- [57] N. Tiwari, S. Kadam, and S. Kulkarni, "Synthesis and characterization of ZnCo₂O₄ electrode for high-performance supercapacitor application," *Materials Letters*, vol. 298, p. 130039, 2021.
- [58] G. P. Kamble, A. A. Kashale, S. S. Dhanayat, S. S. Kolekar, and A. V. Ghule, "Binder-free synthesis of high-quality nanocrystalline ZnCo₂O₄ thin film electrodes for supercapacitor application," *Bulletin of Materials Science*, vol. 42, no. 6, 2019.

- [59] M. Silambarasan *et al.*, "A Facile Preparation of Zinc Cobaltite (ZnCo₂O₄) Nanostructures for Promising Supercapacitor Applications," *Journal of Inorganic and Organometallic Polymers and Materials*, vol. 31, no. 10, pp. 3905-3920, 2021.
- [60] G. Gupta, U. N. Kumar, N. Khatun, T. Thomas, and S. C. Roy, "Comparative Study of Morphological Variation in Bi-functional ZnCo₂O₄ Nanostructures for Supercapacitor and OER Applications," *Journal of Electronic Materials*, vol. 52, no. 5, pp. 3188-3204, 2023.
- [61] K. Aruchamy, A. Balasankar, S. Ramasundaram, and T. Oh, "Recent Design and Synthesis Strategies for High-Performance Supercapacitors Utilizing ZnCo₂O₄-Based Electrode Materials," *Energies*, vol. 16, no. 15, p. 5604, 2023.
- [62] R. Zhang, J. Liu, H. Guo, and X. Tong, "Rational synthesis of three-dimensional porous ZnCo₂O₄ film with nanowire walls via simple hydrothermal method," *Materials Letters*, vol. 115, pp. 208-211, 2014.
- [63] H. Che, A. Liu, X. Zhang, J. Mu, Y. Bai, and J. Hou, "Three-dimensional hierarchical ZnCo₂O₄ flower-like microspheres assembled from porous nanosheets: Hydrothermal synthesis and electrochemical properties," *Ceramics International*, vol. 41, no. 6, pp. 7556-7564, 2015.
- [64] A. Khataee, P. Eghbali, M. H. Irani-Nezhad, and A. Hassani, "Sonochemical synthesis of WS₂ nanosheets and its application in sonocatalytic removal of organic dyes from water solution," *Ultrason Sonochem*, vol. 48, pp. 329-339, Nov 2018.
- [65] J. Vujan, W. Huang, J. Ciganovic, S. Ptasinska, and R. Panajotovic, "Direct Probing of Water Adsorption on Liquid-Phase Exfoliated WS₂ Films Formed by the Langmuir-Schaefer Technique," *Langmuir*, vol. 39, no. 23, pp. 8055-8064, Jun 13 2023.
- [66] R. Sharma *et al.*, "A Thrifty Liquid-Phase Exfoliation (LPE) of MoSe₂ and WSe₂ Nanosheets as Channel Materials for FET Application," *J Electron Mater*, vol. 52, no. 4, pp. 2819-2830, 2023.
- [67] L. Ma, Z. Liu, and Z.-L. Cheng, "Scalable exfoliation and friction performance of few-layered WS₂ nanosheets by microwave-assisted liquid-phase sonication," *Ceramics International*, vol. 46, no. 3, pp. 3786-3792, 2020.
- [68] B. Adilbekova *et al.*, "Liquid phase exfoliation of MoS₂ and WS₂ in aqueous ammonia and their application in highly efficient organic solar cells," *Journal of Materials Chemistry C*, vol. 8, no. 15, pp. 5259-5264, 2020.
- [69] L. Cheng, M. Xu, Q. Zhang, G. Li, J. Chen, and Y. Lou, "NH₄F assisted and morphology-controlled fabrication of ZnCo₂O₄ nanostructures on Ni-foam for

- enhanced energy storage devices," *Journal of Alloys and Compounds*, vol. 781, pp. 245-254, 2019.
- [70] Z. Wang, S. Lu, G. He, A. Lv, Y. Shen, and W. Xu, "In situ construction of dual-morphology ZnCo(2)O(4) for high-performance asymmetric supercapacitors," *Nanoscale Adv*, vol. 1, no. 8, pp. 3086-3094, Aug 6 2019.
- [71] B. Pratap Singh *et al.*, "Solvent Free, Efficient, Industrially Viable, Fast Dispersion Process Based Amine Modified MWCNT Reinforced Epoxy Composites Of Superior Mechanical Properties," *Advanced Materials Letters*, vol. 6, no. 2, pp. 104-113, 2015.
- [72] P. Kar and A. Choudhury, "Carboxylic acid functionalized multi-walled carbon nanotube doped polyaniline for chloroform sensors," *Sensors and Actuators B: Chemical*, vol. 183, pp. 25-33, 2013.
- [73] V. V. Mohan, M. Manuraj, P. M. Anjana, and R. B. Rakhi, "WS2 Nanoflowers as Efficient Electrode Materials for Supercapacitors," *Energy Technology*, vol. 10, no. 3, 2021.
- [74] T. Fatima, S. Husain, J. Narang, M. Khanuja, N. P. Shetti, and K. R. Reddy, "Novel tungsten disulfide (WS2) nanosheets for photocatalytic degradation and electrochemical detection of pharmaceutical pollutants," *Journal of Water Process Engineering*, vol. 47, p. 102717, 2022.
- [75] X. Xiao, B. Peng, L. Cai, X. Zhang, S. Liu, and Y. Wang, "The high efficient catalytic properties for thermal decomposition of ammonium perchlorate using mesoporous ZnCo(2)O(4) rods synthesized by oxalate co-precipitation method," *Sci Rep*, vol. 8, no. 1, p. 7571, May 15 2018.
- [76] K. Prasad, G. R. Reddy, and B. D. P. Raju, "Surfactant assisted morphological transformation of rod-like ZnCo2O4 into hexagonal-like structures for high-performance supercapacitors," *Indian Journal of Science and Technology*, vol. 14, no. 7, pp. 676-689, 2021.